RSC Advances

REVIEW

View Article Online
View Journal | View Issue

Cite this: *RSC Adv.*, 2018, **8**, 30125

Recent advances in syntheses, properties and applications of TiO_2 nanostructures

Imran Ali, *[ab] Mohd Suhail,[b] Zied A. Alothman[c] and Abdulrahman Alwarthan[c]

TiO_2 is a compound of great importance due to its remarkable catalytic and distinctive semiconducting properties. It is also a chemically stable, non-toxic and biocompatible material. Nano TiO_2 is strong oxidizing agent with a large surface area and, hence, high photo-catalytic activities. With low production cost and a high dielectric constant, it is an inexpensive material. It can be prepared by diverse procedures such as solution and gas phase procedures. Nowadays, TiO_2 is being used frequently for photo degradation of organic molecules and water splitting for hydrogen generation. Most important applications include purification, disinfection of waste water, self-cleaning coatings for buildings in urban areas and the production of the green currency of energy (hydrogen) by splitting water. The review describes the advances in the syntheses, properties and applications of TiO_2 nano structures. Besides, efforts are also made to discuss the working mechanism and future challenges and perspectives.

Received 2nd August 2018
Accepted 20th August 2018

DOI: 10.1039/c8ra06517a

rsc.li/rsc-advances

1. Introduction

Nowadays, nano-structured materials are an important area of research owing to their several unique characteristic features. Among all the transition metal oxides, TiO_2 nano-structures are the most attractive materials in modern science and technology. TiO_2 has been widely used commercially in doughnuts, cosmetics, pigments,[1] catalysts, sunscreens,[2,3] solar cells,[4] water splitting *etc.* TiO_2 is being used in plastics, paints, varnishes, papers, medicines, inks, medications, toothpaste, food products, and industries.[5–10] In 1972 first of all, Fujishima and Honda[4] reported photo-assisted water splitting under UV light on a TiO_2 photo anode as a semiconductor.[4,11,12] The diverse claims can be separated into "environmental" and "energy" groups, several of which depend on the TiO_2 properties itself as well as on the changes of the TiO_2 material host (*e.g.* with organic and inorganic dyes). In previous years, the research activity expansion has been observed in nanotechnology and nanoscience.[13–17] On the modification, preparation and properties of nano-materials, a significant amount of research, reports and reviews have been published recently[4,11–40] to know and précis the progress in this field. TiO_2 nanostructures in various forms, among the unique characteristics of nano-materials, are gaining broader applications due to their size-related characteristics. For nanometer scale TiO_2 the energy band structure becomes discrete due to its surface, photochemical and photo physical properties. Consequently, several works have focused on nano crystalline TiO_2 syntheses with a high surface area. As a photocatalyst,[15,16,27] TiO_2 nanostructures have drawn much attention and are projected to show a significant role in serving to resolve several pollution and environmental problems. Thus, using TiO_2 for H_2 production and photo-assisted water splitting devices offers a way for hygienic and low price production of hydrogen by solar energy.[13,41]

This review aims to give an inclusive data on the advances in TiO_2 based nanostructure, recent investigation and the development efforts, which tack energy and environmental challenges in consideration. Besides, the crystal structure, optical, electrical/electronic and adsorption, surface area, porosity properties of TiO_2 nanostructure are discussed. The procedures of preparations, fabrications (nanoparticles, nanorods, nanowires, and nanotubes), the conditions of syntheses and accountability for regulation of titanate nanostructures morphology are also discussed. TiO_2 nanostructures applications in electrocatalysis, environment and energy challenges are also highlighted. Finally, the mechanism of action and future challenges are also highlighted.

2. Properties of TiO_2 nanostructures

2.1 Crystal structure of TiO_2

Titanium dioxide [titanium(IV) oxide or titania] has a molecular formula TiO_2 with 79.87 as molecular weight. TiO_2, a non-toxic material, chemically stable, biocompatible and strong oxidizing agent (with large surface area) has very high photocatalytic activity. It is an inexpensive material with high dielectric constant and low production cost. TiO_2 crystal exists in three

[a]*Department of Chemistry, College of Sciences, Taibah University, Al-Medina Al-Munawara – 41477, Saudi Arabia. E-mail: drimran.chiral@gmail.com; drimran_ali@yahoo.com*

[b]*Department of Chemistry, Jamia Millia Islamia, Central University, New Delhi, India*

[c]*Department of Chemistry, College of Science, King Saud University, Riyadh 11451, Kingdom of Saudi Arabia*

common polymorphs in nature *i.e.* brookite, anatase, rutile,[42,43] and some few common structures of TiO_2 II *i.e.* columbite,[44] TiO_2 III: baddeleyite,[45,46] TiO_2 (R) (ramsdellite),[47] TiO_2 (B) (monoclinic)[48] and TiO_2 (H) (hollandite).[49]

Rutile is the most thermodynamically constant among the different polymorphs structures.[50] From 400 to 1200 °C, it's critical temperature can vary which depends on the grain impurities and size.[51] The optical and electrical properties and crystal structural of rutile, brookite and anatase are given in Table 1.[51–63] These are discussed in the following paragraphs.

2.2 Rutile

In a tetragonal structure, with 6 atoms per unit cell (Fig. 1), rutile is the most stable having TiO_6 octahedron showing a slight orthorhombic distortion.[64–66] Rutile phase is stable while at these conditions TiO_2 converts thermodynamically into auspicious phase.[67] For unit sizes > 14 nm, rutile phase becomes more stable than anatase.[68] Predominantly, the crystals of natural rutile exhibit (110) surface.[42] This surface is the most stable stoichiometric rutile surface.[69] In the unit cell of rutile, 4 oxygen atoms form a partial octahedron about Ti[70] while 2 titanium atoms (at [0, 0, 0] and $\left[\frac{1}{2}, \frac{1}{2}, \frac{1}{2}\right]$) positions, separately are available. Distinctly, octahedron is linked to 10 near octahedra, out of which 2 parts an edge and eight share a bend with it. The octahedral edge shared are aligned along [001] direction as shows in Fig. 1.[70]

2.3 Anatase

TiO_6 octahedron distortion is significantly large for anatase phase while TiO_2 has a tetragonal structure, hence, the symmetry of anatase is lower than orthorhombic (Fig. 1).[70] The energy change between these 2 phases is minor closely (~2 to 10 kJ mol^{-1}).[71] At 0 K, the rutile phase is not more thermodynamically constant than anatase. The unit cells of anatase

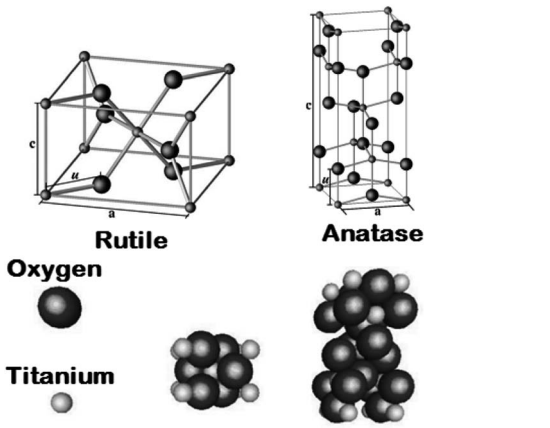

Fig. 1 Crystal structures of the rutile and anatase phases of TiO_2. Small spheres represent Ti atoms, large spheres represent oxygen atoms.

contain 4 titanium atoms (at $\left[\frac{1}{2}, \frac{1}{2}, \frac{1}{2}\right]$, [0, 0, 0], $\left[-\frac{1}{2}, 0, -\frac{1}{4}\right]$ and $\left[0, \frac{1}{2}, \frac{1}{4}\right]$) and 8 oxygen atoms, which form a partial TiO_6 octahedron around Ti;[70] with division of 4 edges of each octahedron.

2.4 Brookite

It is one of the 3 naturally occurring polymorphs of TiO_2, which belongs to orthorhombic crystal system. It contains a larger cell volume with 8 TiO_2 groups per unit cell (Fig. 2).[53] Brookite is also the least dense form compared to anatase and rutile.[65] Besides, it displays photocatalytic activity.[72] Liu *et al.*[73] investigated principled metal free photocatalytic water splitting. For this investigation the authors modified these surfaces by high pressure. Before and after modification, water splitting on usual anatase single crystal facets and on wafer slices of the [001] plane was investigated. Fig. 3 shows phase transition in TiO_2

Table 1 Comparison of the crystal structural, optical and electrical properties for TiO_2 nanostructures

Properties	Rutile	Anatase	Brookite
Crystal structure	Tetragonal	Tetragonal	Orthorhombic
Lattice constant (Å)	$a = 4.5936$	$a = 3.784$	$a = 9.184$
	c =2.9587 (ref. 312)	$c = 9.515$ (ref. 312)	$b = 5.447$ (ref. 312)
			$c = 5.154$
Space group	$P42/mnm$[52]	$I4_1/amd$	$Pbca$
Molecule (cell)	2	2	4
Volume/molecule (Å^3)	31.21 (ref. 54)	34.061	32.172
Density (g cm^{-3})	4.13	3.79	3.99
Ti–O bond length (Å)	1.949 (4)[53]	1.937 (4)	1.87–2.04
	1.980 (2)	1.965 (2)	
O–Ti–O bond angle	81.2°	77.7°	77.0–105°
	90.0°	92.6°	
Band gap at 10 K	3.051 eV (ref. 54)	3.46 eV (ref. 313)	
Static dielectric constant (ε_0, in MHz range)	173 (ref. 314 and 315)	48 (ref. 55)	
High frequency dielectric constant, ε_∞ ($\lambda = 600$ nm)	8.35 (ref. 56)	6.25 (ref. 57)	
Nature of conductivity at room temperature (undoped)	n-type semiconductor[58–75]		
Mott transition	Not observed[60]	Observed[313]	
Electron effective mass	9–13 m,[61] 10–30 m,[62] 12–32 m[63]	~1 m (ref. 313)	

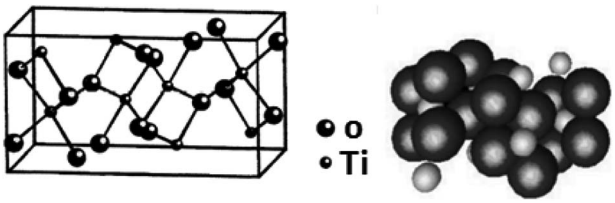

Fig. 2 Lattice structure of brookite TiO_2.

with the change in pressure and temperature.[74] The temperature for transformation can be improved by accumulation impurities into TiO_2. Anatase phase for powder samples containing V, Mo, & W respectively completely disappeared[75] at temperature about 530, 680, and 830 °C.

2.5 Optical properties of TiO_2

In the range from IR to visible spectra, the rutile is more anisotropic than anatase. Contrarily, anatase shows important anisotropy in the band gap region.[76] At about 0.75 to 1.18 eV (ref. 77–80) for rutile, a blue color appearance dependent on the amount of reduction of TiO_2, arises from the visible part infrared absorption band peaking. The blue color appearance in IR has also been observed in anatase too.[81,82] Besides, at 3.0 eV an oxygen vacancy causing a yellow color is a color center.[81]

2.6 Electrical/electronic properties of TiO_2

The electrical/electronic properties of TiO_2 nanostructures are dependent on the crystallographic directions. Titanium dioxide nanostructure (titania) is an important photocatalytic material, which exists in to 2 chief polymorphs *i.e.* rutile and anatase with tetragonal coordinations. Table 1 shows the several TiO_2 electrical properties. A semiconductor, TiO_2 has high resistivity ($\sim 10^{15}$ Ω cm),[83] titanium interstitials and bulk oxygen vacancies. These are considered to generate low electron donor levels that donate to the electric conductivity of TiO_2.[84]

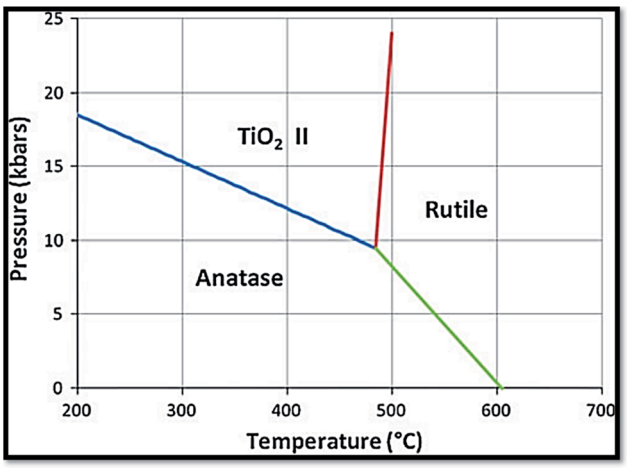

Fig. 3 Reaction boundaries of phase transitions in TiO_2.[74]

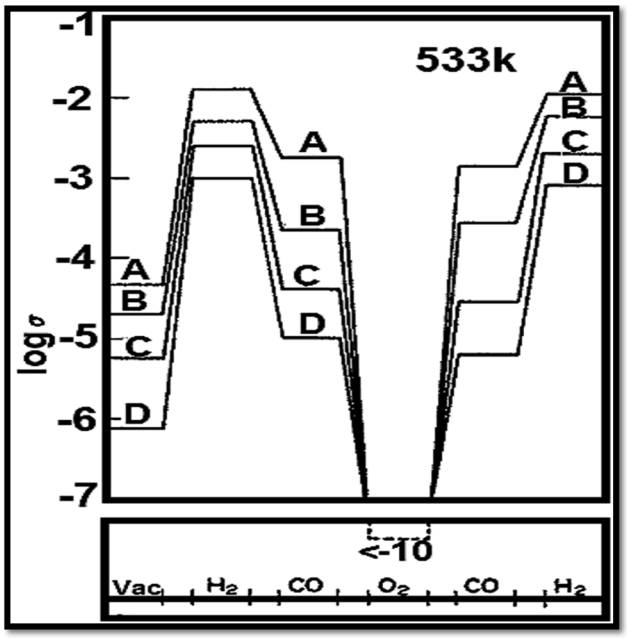

Fig. 4 Influence of gas cycle of sequence on electrical conductivity of 0.5% Pt/TiO_2 doped with (A) W^{6+} (B) Ta^{5+} (C) undoped and (D) Mg^{2+}.[85]

Vacancies for oxygen are the main fault in TiO_2.[70] The absence of oxygen introduces electrons excess in the solid ensuing in a rise of conductance of electricity.[70] Fig. 4[85] shows the influence of gas cycle of sequence on electrical conductivity of 0.5% Pt/TiO_2 doped with (A) W^{6+} (B) Ta^{5+}(C) undoped and (D) Mg^{2+}. Another thing to be added is that Nb (niobium) or tantalum atoms act as electron donors[86] when incorporated into TiO_2. Besides, Nb (niobium) or tantalum atoms increase the electrical conductivity. On the other hand, chromium, manganese, and iron act as electron acceptors,[87] decreasing or increasing the TiO_2 electrical conductivity. On the ratio between the oxygen vacancy concentration and their concentration, the augment or reduction in electrical conductivity depends.[88] To the electrical conductivity, the point defects typed imperfection plays a crucial role. It is reported that the ionization energies for titanium interstitials[89] is 0.007–0.08 eV. To the electronic conduction, the contribution of oxygen vacancies is also important.[90] Several reports recommended the presence of both phenomena, with an activation energy of carrier generation around 4 meV.[91]

After studying the formation energies and the electronic states of 4 types of lattice point defects in rutile, it was found that in the forbidden band, the existence of vacancy for oxygen leads to a deep donor defect level. Moreover, to establish that the band gap is ~2.86 eV, the band building of the pure rutile TiO_2 was studied.[92] The valence band (VB) of wide gap rutile and anatase are formed by O_{2p} states, while titanium 3d states forms the conduction band (CB).[70] On these states, the detailed calculations can be found.[45] Recently, several researches have been reported that the electronic structure of rutile bulk can also be described by means of additional techniques used in the experiment such as electrical resistivity, electroabsorption,[93,94]

photoconductivity and photoluminescence,[95,96] X-ray absorption spectroscopy (XAS),[97–102] resonant Raman spectra[96,103] and photoelectrochemical analysis.[58,104]

3. Synthesis of TiO_2 nanostructures

There are some methods of making TiO_2 nanostructures. Gas phase and solution routes methods are the main ones. The solution route is able to coat complex shapes, to govern on stoichiometry, and preparation of composite materials. The presence of carbon as an impurity is an expensive precursor, and long processing times are the difficulties of solution route. There are two methods of synthesis (i) physical and (ii) chemical methods. Both methods have disadvantages and advantages. Physical procedures produce large quantities of material, but their resolution is inadequate to nanometers. The chemical procedures can approach the atomic layer limit[105] through the preparation of minor (*e.g.*, <100 nm and often <10 nm) structures. Hence, at a smaller scale, chemical procedures are typically completed.

3.1 Solution procedures

3.1.1 Sol gel route. In materials science and ceramic engineering, a wet-chemical technique widely used is sol–gel process. The advantage of sol–gel process is inexpensiveness. With sol–gel method, nanostructured TiO_2 has been synthesized from titanium precursor hydrolysis. Usually, this method involve an acid catalyzed hydrolysis of titanium(IV) alkoxide tracked by condensation.[106–119] This process includes 4 steps *i.e.* hydrolysis, polycondensation, drying and thermal decomposition. The sol–gel procedure includes the metal alkoxides usage, which suffer hydrolysis and condensation polymerization reactions to give gels as shown in these equations.[120]

Hydrolysis:

$$Ti(OR)_4 + 4H_2O \rightarrow Ti(OH)_4 + 4ROH \quad (1)$$

Condensation:

$$Ti(OH)_4 \rightarrow TiO_2 + 2H_2O \quad (2)$$

where, R = ethyl, iso-propyl, *etc.* For the change of liquid sol into a solid gel phase, the whole polymerization leads to loss of solvent. The sol particles size depends on the composition of solution, temperature and pH.[20] Ti–O–Ti chains development is preferred with little amount of water, additional titanium alkoxide in the reaction combination and stumpy hydrolysis rates.

The advantages of sol–gel method are as follows:

- Product homogeneity.
- Good rheostat above powder particle shape and size and size distribution.
- Easiness of manufacturing multi-component materials.
- No particular apparatus with low price.
- Low processing temperature.
- Synthesis of films with high photocatalytic activity.

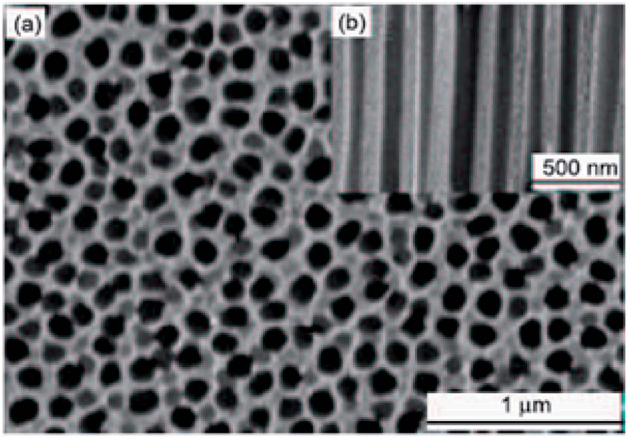

Fig. 5 SEM of AAM template, (a) top and (b) side views.

Utilizing sol–gel template method, the syntheses of TiO_2 nanotubes, nanorod and nanowires has been reported. This synthesis was carried out from the porous anodic alumina membranes (AAMs), supramolecular template and organogel. The first step for synthesis of nanorod is tumbling porous AAMs into a warmed TiO_2 sol following by drying and heating processes.[121] Ghamsari and colleagues[122] synthesized TiO_2 nanorod by sol–gel Template Process. Briefly, the porous anodic alumina of 60 μm in thickness and pores of 100 nm in diameter were used as templates.

Fig. 5 and 6 show SEM images of AAM template and TiO_2 nanorods grown in the AAM template. By changing the dipping time, nanorods length can be changed. An individual TiO_2 nanorods picture is shown in Fig. 6(b). Through the full length of the rods and continuous yet the rode is uniform. To obtain the nanowire arrays of TiO_2, electrophoretic deposition of TiO_2 colloidal suspensions can be used into the pores of an AAM.[123] At room temperature; in another procedure; titanium tetraisopropoxide (TTIP) is dissolved in ethanol followed by the

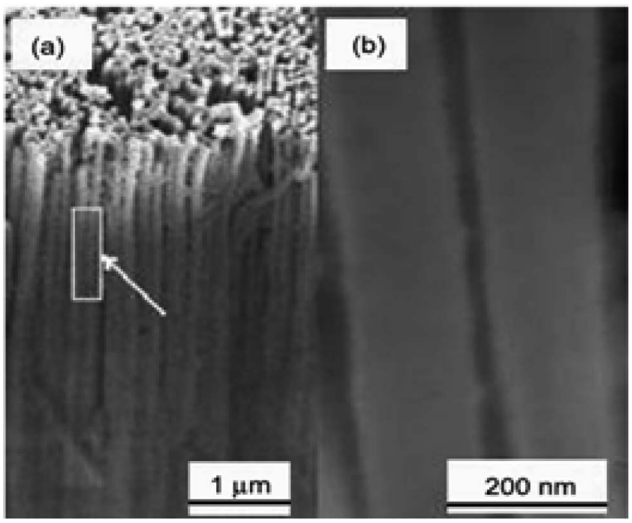

Fig. 6 SEM of TiO_2 nanorods growth in AAM template, (a) low magnification image, (b) high magnification image.[123]

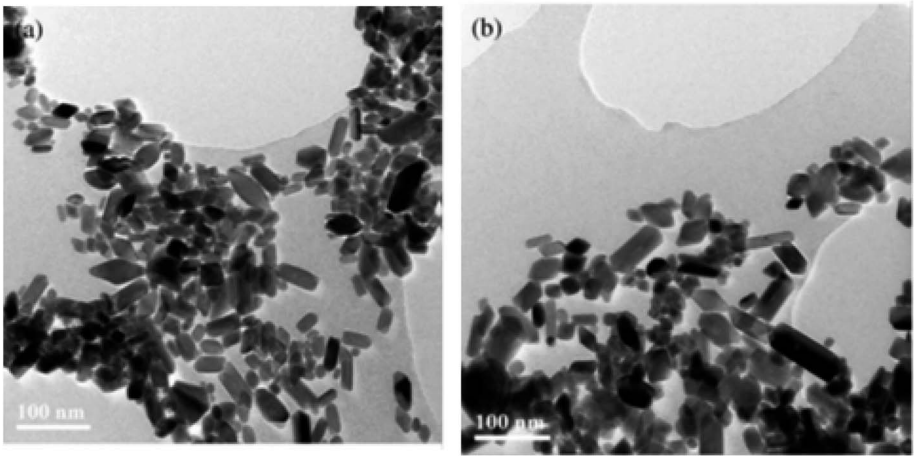

Fig. 7 TEM images of TiO_2 nanoparticles after hydrothermal treatment of TBA peptized gel at (a) 210 °C and (b) 270 °C.[133]

addition of glacial CH_3COOH (mixed with demineralised water and EtOH) using HNO_3 as pH 2–3 controller. AAM is used as the cathode and platinum as an anode. TiO_2 nanowires are obtained after dissolving AAM template in 5% NaOH solution. Using titanium butoxide, titanium isopropoxide [TIPO] and titanium tetrachloride; as Ti precursors in HCl solution; have been synthesized.[124] Nanotubes were also synthesized by Kasuga and colleagues[125–127] using sol–gel method with innermost and outside diameters of approximately 5 and 8 nm, respectively. The spine designed products were nanotubes.

3.1.2 Hydrothermal procedures. Hydrothermal syntheses are promising procedures to gain titania nanocrystalline particles. The hydrothermal process is effective to attain the crystalline phase at lower temperatures. Hydrothermal is broadly used for the manufacture of minor units in the ceramics industry. Generally, hydrothermal synthesis is known as crystal synthesis or crystal growth. Below 300 °C, the hydrothermal synthesis is usually carried out. 374 °C is the critical temperature and 22.1 MPa is the critical pressure of water under supercritical conditions.

Some studied indicated application of hydrothermal method to prepare TiO_2 nanoparticles.[128–132] To synthesize TiO_2 nanoparticles, hydrothermal treatment of titanium precursor (peptized precipitates) was also used.[129] Besides, reaction of hydrothermal of titanium alkoxide under acidic ethanol–water solution was also used to prepare TiO_2 nanoparticles. Under EtOH–H_2O environment, TiO_2 nanoparticles synthesized were mainly primary structures of anatase. The sizes of the units were in range of 7–25 nm. Besides, TiO_2 nanoparticles[133] were synthesized using hydrothermal method. With increasing stirring for 45 minutes into distilled water at 1 : 4 volume ratio, 0.5 M solution of titanium butoxide $Ti(OBu)_4$ in 2-propanol was gradually added. To prepare nanoparticles for further examination, the gels prepared were treated hydrothermally. TEM images of TiO_2 nanoparticles prepared using hydrothermal method are shown in Fig. 7.

Vijayalakshmi and Rajendran[134] synthesized TiO_2 nanoparticles using hydrothermal method by making a water solution of titanium. This solution was made by mingling one molar stoichiometric ratio of TTIP in 50 mL deionized water. TiO_2 nanowire in the solutions of 10 to 15 M sodium hydroxide were synthesized; using TiO_2 white powders; without stirring within an autoclave at 150–200 °C for 24–72 h by Zhang and colleagues.[135] Fig. 8 shows SEM and TEM images of nanowires of TiO_2 prepared by Zhang and colleagues.[135] Titania nanotubes[136] were synthesized *via* hydrothermal process. TiO_2 powders were heated at 20–110 °C for 20 h. TiO_2 nanotubes achieved were washed using a dil. HCl aqueous solution and deionized water. With NaOH aqueous solution, raw TiO_2 material was treated. Besides, titania nanotubes[137] were synthesized *via* hydrothermal. 5.0 g anatase TiO_2 nanopowders were mixed with 180 mL 10 M NaOH in a perfluoroalkoxy (PFA) bottle and stirred for 1 h. The resultant precipitate was separated by centrifugation after hydrothermal reaction. Until pH value reached approximately 7, precipitate was rinsed with

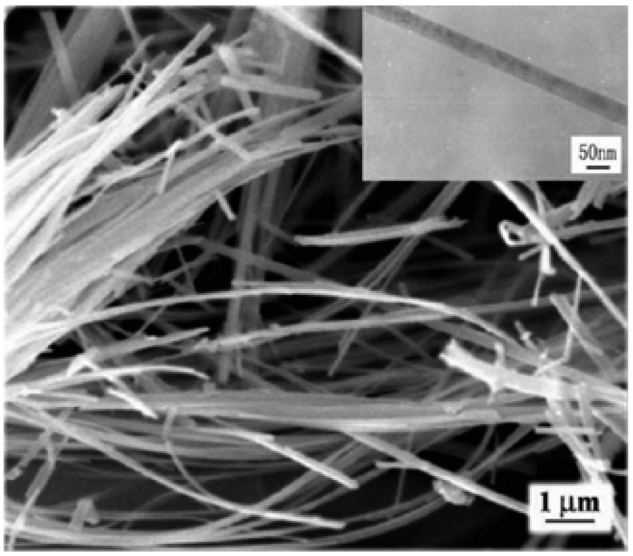

Fig. 8 SEM images of TiO_2 nanowires and a TEM image of a single nanowire prepared by Zhang and colleagues.[135]

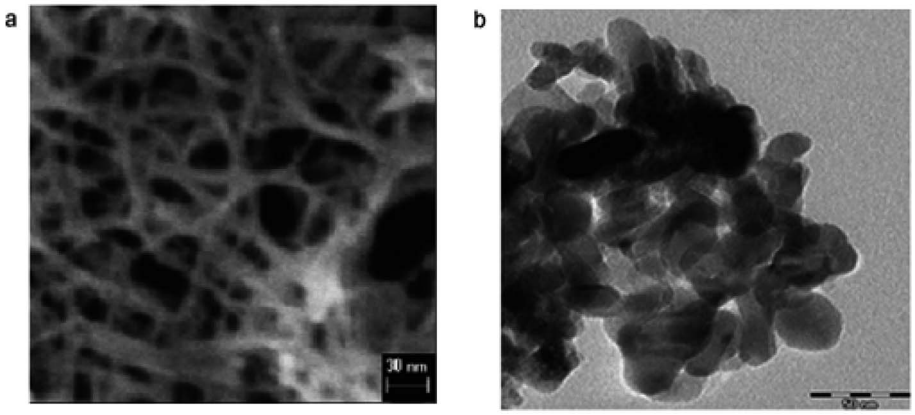

Fig. 9 Electron microscopy images of (a) titania powders and (b) titania nanotubes.[312]

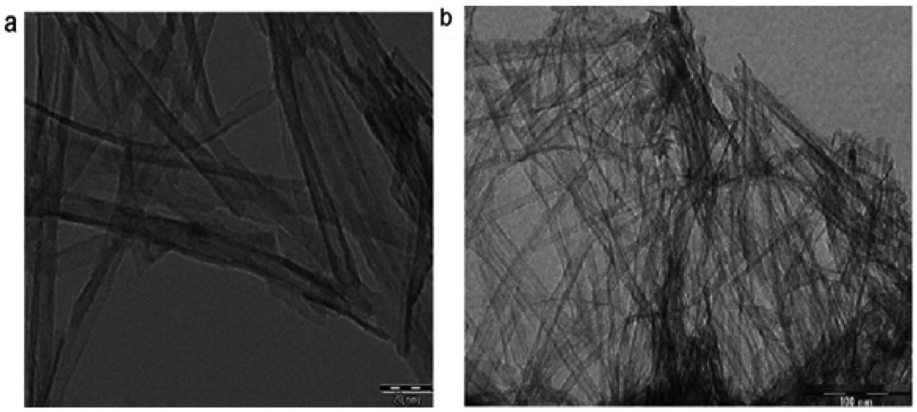

Fig. 10 TEM images of titania nanotubes at (a) low magnification and (b) high magnification.[338]

diluted HCl and demineralised water several times. Fig. 9 shows electron microscopy pictures of titania nanotubes and titania powders. Fig. 10 indicates the TEM pictures of TNTs; revealing that the TNTs have tubular, hollow and open structures. 3–6 nm is the inner diameter size of the TNTs and 1.9 nm is the average wall thickness. Besides, some other studies for syntheses of TiO_2 nanowires by hydrothermal are also available.[110–115]

3.1.3 Electrochemical procedures. To produce advanced thin films such as superlattice, epitaxial, nanoporous and quantum dot ones by anodization, electrochemical procedures provided a diversity and low temperature approach. The distinctive states of the films are measured by electrolysis parameters such as temperature, current density, potential and pH.[138] In a typical process, the conducting piece (undergoing anodization) is positioned in an electrolytic bath serving as anode. The cathode was a rod of platinum. From electrolyte to positive anode, at power supply the electrons are forced. Drifting through the power source, the electrons return to cathode. With hydrogen ions, these electrons react due to which bubbles off hydrogen gas are occurred. If oxide film is porous, the primary determinant is the electrolyte composition. Fig. 11[139] shows a representation of an electrochemical anodization cell.

In 2001, TiO_2 nanotube arrays fabrication through anodic Ti oxidation was reported first time.[140] Advanced studies engrossed on extension of morphology,[141] length, pore size[142] and wall thickness[143] of the nanotube were carried out. Fig. 12[144] shows SEM of TA6V anodised in CA electrolyte under 5 V for 20 min. The usage of different electrolytic diluents permitted the architecture control from well detached, standalone nanotubes to tightly packed arrays. The wall thickness of typical nanotubes ranged from 5 to 30 nm, with 20 to 350 nm pore size and 0.2 to 1000 mm length. Zwilling and co-workers[144] used fluorinated electrolyte to produce a porous surface of TiO_2 films

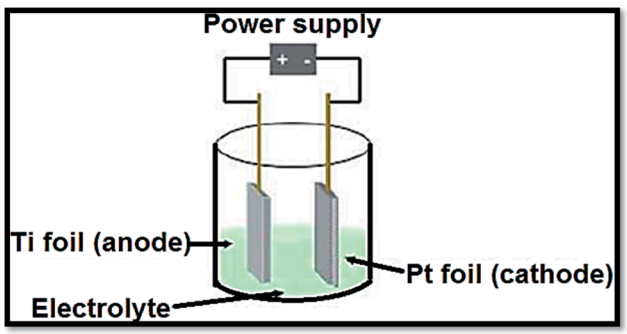

Fig. 11 Depiction of an electrochemical cell in which the Ti samples are anodized. Fabrication variables include temperature, voltage, pH and electrolyte composition.

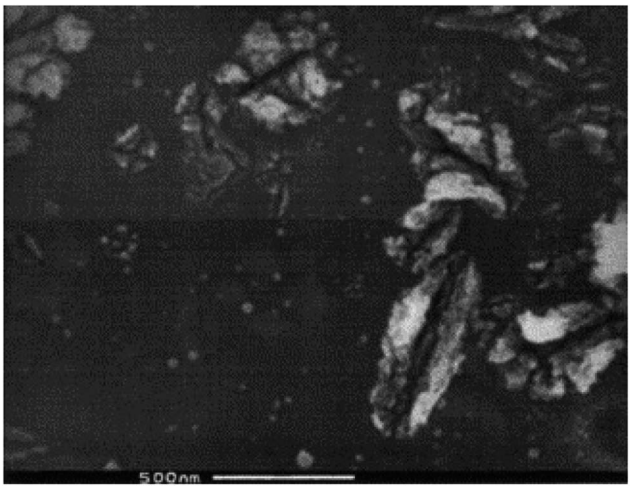

Fig. 12 Scanning electron micrograph of TA6V anodised in CA electrolyte.[144]

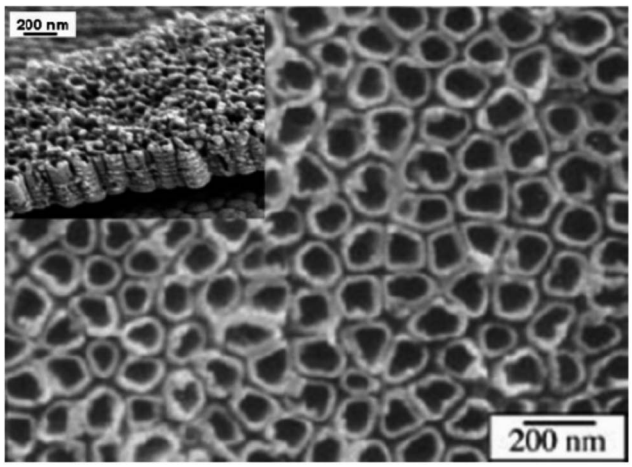

Fig. 13 SEM images of TiO_2 nanotubes prepared with anodic oxidation.[159]

via electrochemically anodization of titanium. Shimizu *et al.*[145] reported that dil. H_2SO_4 could be used to bond porous TiO_2 thin films. Yamamoto *et al.*[146] observed that the act of dye-sensitized solar cell device was better by cathodically electro-synthesized TiO_2 films; having sealed commercial Degussa P25 nanoparticles. Anodization or anodic oxidation of titanium foils was conducted by Patermarakis *et al.*[147] Platinum and titanium were used as cathode and anode. Using formamide–water mixtures (having fluoride ions), Shankar and co-workers[148] studied the effect of five dissimilar cationic species on development of TiO_2 nanotube array.

In 2006, Ruan and co-workers[149] synthesized titania nanotube by titanium anodization in an electrolyte. In 2006, nanotube arrays of protracted length from DMSO electrolytes was described by Paulose and co-workers.[150] The importance of diethylene glycol (DEG) for nanotube array synthesis was reported by Yoriya and co-workers.[151] These authors investigated tube formation. The necessity of tube separation and crystallization in the DEG-based electrolytes were required. The benefit of TiO_2 nanotubes produced by anodization is readily attachment capability in a perpendicular orientation onto the substrate; improving electron transfer pathways as compared to the non-oriented structure.[152] In one study, glycerol pH and water (75–25, v/v) electrolyte having 0.5% NH_4F were modified using H_2SO_4.[153] The length of nanotube was 950 nm on adjusting pH 5.6 by H_2SO_4. Nanotubes of 16 mm were found by anodizing at 20 V for 8 h after adding of 0.1 M CH_3COONa by maintaining pH at 5.6. TiO_2 nanostructured as photoanodes were prepared by nanotubes of TiO_2 by anodic oxidation of foil of titanium[140,154–156]. In a model experimentation, a plate of clean titanium was anodized in a 0.5% hydrogen flouride solution under 10–20 V for 10–30 min. The counter electrode used in the experiment was platinum. Crystallized TiO_2 nanotubes were obtained by annellation of plate of anodized Ti at 500 °C for 6 hours in oxygen.[157] The diameter and length of TiO_2 nanotubes may be optimized with the utilized potential between 1.0 and 25.0 V in optimized phosphate/HF electrolytes.[158] SEM pictures of TiO_2 nanotubes produced with this approach are shown in Fig. 13.[159] For the first time, H generation efficiency, phase evolution and electrochemical synthesis of anatase, anatase–rutile and anatase–rutile–brookite (ARB) TiO_2 nanotubes was reported Preethi *et al.*[160] The samples tubular morphology was confirmed by TEM and SEM.

3.2 Gas phase procedures

3.2.1 Chemical vapor deposition. The vapor deposition processes to form coatings to alter the mechanical, electrical are normally used. Also, these methods can be castoff to produce free-stand bodies, fibers and films, or to form fused materials. Recently, chemical vapor depositions have received great attention in the manufacture of nanomaterials. These processes occur in a vacuum space and if chemical reaction doesn't occur, these processes are called physical vapor deposition (PVD). In this process, gases must be heated by suitable thermal. By using liquid precursor and titanium tetraisopropoxide (TTIP), pyrolysis in a mixed gases (consisting of helium/oxygen atmosphere) leads to prepare bushy crystalline of TiO_2 films with sizes below 10 nm.[161] Ayllon *et al.*[162] described the synthesis of amorphous nanoparticles of TiO_2. Pradhan, *et al.*[163] prepared nanorod arrays of TiO_2 with a length of 0.5–2 μm and a diameter of about 50–100 nm (Fig. 14). Metal organic CVD was used by the authors on a WC-Co substrate using (TTIP) as the precursor. Similarly, on the particle size distribution of aerosol particles prepared by gas-phase chemical reactions, Okuyama and colleagues[164–166] described the effects of the primary concentration of TTIP vapor and temperature profile of the furnace. They found that in the controlled cylindrical furnace, the thermal decomposition of TTIP vapor led to form 10–60 nm sized ultrafine TiO_2 nanoparticles. Likewise; using TTIP as precursor; the formation of TiO_2 nanoparticles reinforced on porous silica gel (60–100 mesh) *via* metalorganic chemical vapor deposition MOCVD process was reported by Ding and colleagues.[167] A tubular furnace controlled the reactor temperature. Pretreatment of the support materials, CVD reaction and calcinations process were

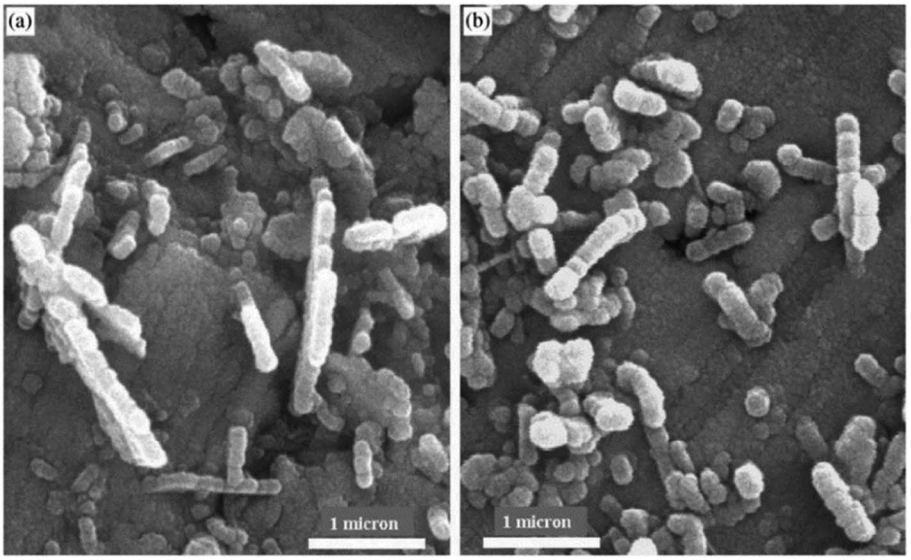

Fig. 14 SEM micrograph of TiO_2 nanowires deposited without NH_3 at 500 °C; (a) with 800 sccm argon flow, and (b) with 500 sccm argon flow.[163]

involved in the synthesis of TiO_2 nanoparticle/silica gel photocatalyst. Contrarily, the fabrication of TiO_2 nanorods grown on fused silica substrates was reported by Wu *et al.*[168] Directly, the nanostructures of TiO_2 were grown on the substrates. The only one crystalline anatase and rutile TiO_2 nanorods were formed, respectively, when the temperature ranged between 630 and 560 °C at a pressure of 5 torr. Furthermore, for preparing of TiO_2 nanomaterial, the foregoing chemical vapor deposition approaches were also used. These included electrostatic spray hydrolysis,[169] diffusion flame pyrolysis,[170] ultrasonic spray pyrolysis, thermal plasma pyrolysis[171–173] laser-induced pyrolysis[174,175] and ultra-sonicated hydrolysis *etc.*

3.2.2 Physical vapor deposition. Among several techniques for the syntheses of TiO_2 nanowires, primary PVD procedures include ion implantation.[176–178] Before growth of TiO_2 nanowires, a layer of Ti nanopowders deposited on the substrate was also reported by this group.[176,177] These authors used gold as catalyst.[176] Fig. 15 displays a model SEM image of nanowires of TiO_2 made by physical vapor deposition method.[176] Xiang *et al.*[179] reported deposit of TiO_2 nanowire on a Si substrate *via* thermal evaporation of Ti powder in a precise furnace. These authors molded SiO_2/TiO_2 shell–core nanostructures by monitoring the preparation surroundings such as the time of reaction and the substrate position.[179] On a Si substrate, a two-steps thermal evaporation technique was used to grow TiO_2 nanowires. By a radio frequency coil, Ti powder was heated inside a quartz reactor under mixed gases composed of Ar-diluted O_2 atmosphere.[177–180]

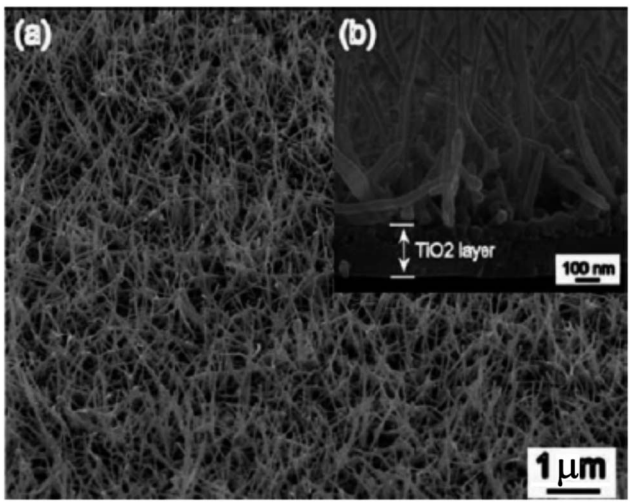

Fig. 15 SEM images of the TiO_2 nanowire arrays prepared by the PVD method.[176]

4. Applications of TiO_2 nanostructures

TiO_2 nanostructures have several advantages making them as the most important existing resources with promising usage in the deferent areas. These unique features of TiO_2 include electronic and short diffusion path. Generally, TiO_2 nanomaterials are wide band gap semiconductors containing E_g-values ranging from 3.0 to 3.2 eV with high absorption in the UV region. Titanium dioxide (nanomaterial) is used an important material in high-tech applications. It is the most bio-compatible material. Its optical and biologically properties are responsible for UV protection applications.[181–184] As implant materials, TiO_2 nanostructures are successfully used for dental, orthopedic and osteosynthesis applications.[185] TiO_2 suitable for optical applications.[70] Besides, photochromism has also been observed in single crystal iron doped rutile.[186] Today, the largest practical research on TiO_2 is its use for photo assisted organic molecules degradation.[187] The applications utilizing this process are purification of waste water, disinfection and self-cleaning coatings in urban areas buildings. The following sub-sections describe different applications of nano TiO_2 structures.

4.1 Photocatalytic applications

Various semiconductor materials such as WO_3, ZrO_2, $BiVO_4$, Fe_2O_3 and $NaTaO_3$ have been developed and showed photocatalytic activities over the past few periods. Among of these, TiO_2 is the most photo-catalytically active material used for water splitting as well as decomposition of organic materials.[65,188–190] Hydrogen is environmental friendly and clean and, hence, it is considered as the future fuel. Numerous studies have been developed to produce hydrogen by splitting water. First of all in 1972, Fujishima and Honda[4] reported the photocatalytic splitting of water in the occurrence of a TiO_2 catalyst. These materials have also been used to kill bacteria in water treatment[191] and tumor cells in cancer treatment.[14,192] Some reviews are available on the photocatalytic mechanisms.[11,16,24,33] By the absorption of photon hv_1, the photocatalytic mechanism is initiated manufacturing an electron–hole pair on the surface of TiO_2 nanoparticle. An electron is encouraged to the conduction band (CB) with formation of a positive hole with the valence band (VB). One or more radicals or intermediate species involved in this photodecomposition process play a crucial role in the photocatalytic mechanisms of reaction. The different factors play significant roles in controlled photocatalytic activities of semiconductors. With constant adsorbents density on the surface, the semiconductors having large surface area lead to faster reactions on the surface.[193]

The size of titanium dioxide particles is much correlated to the fraction of surface located atoms. Due to the decrease in particles dimensions, the atomic fraction enhancing the catalytic activities on the surface increases. The band gap energy depends on the size of nanoparticle. It increases with decreasing nanoparticle sizes, which can be exploited in the optimization of redox potential. The electrons in transmission band and the holes in valence band allow photoredox reactions easily. For high photocatalytic activity, the band gap permits only UV light to be proficiently used. Kormann and colleagues[112] investigated the decomposition of 2-propanol using different sizes of TiO_2 nanoparticles. The authors observed that photocatalytic activities of 7.0 nm particles were 1.6 times better than 15–30 nm size.

Wang *et al.*[194] studied the decomposition of chloroform by TiO_2 nanoparticles. They prepared TiO_2 nanoparticles with different size particles and observed the best size of TiO_2 nanoparticles for chloroform photocatalytic decomposition. By decreasing particle size from 21 to 11 nm, an enhancement in activity was observed. Contrarily, by reducing to 6 nm, the activity decreased completely. The authors concluded that the optimal particle size was about 10 nm for this reaction. In different types of TiO_2 nanomaterials, TiO_2 nanorods, mesoporous TiO_2 and nanotubes have revealed high photocatalytic performances under the appropriate circumstances.[195–197] Rhodamine B was oxidized by mesoporous TiO_2 by Peng *et al.*[196] On the oxidation reaction of desired materials, TiO_2 mesoporous showed significant activity. The nanotubes of TiO_2 treated with H_2SO_4 solutions were prepared by Yang *et al.*[197] The authors observed that the TiO_2 nanotubes treated with different concentration of H_2SO_4 solutions showed photocatalytic activities for degradation of acid orange II. It was due to small particles having high specific surface areas of TiO_2 nanotubes after treated with H_2SO_4 solution.

To improve the photocatalytic activities under UV irradiation, metal doping TiO_2 nanomaterials have been primarily studied. In current years, wide research work has attentive on visible light tempted photocatalysis by metal doped semiconductor for improved photocatalytic act on the various organic pollutants degradation.[196–202] As potential dopants, several metal ions including iron[203–205] nickel[206,207] vanadium[208] chromium[209] platinum[210] ruthenium and cobalt ions[211] have been investigated. There are contradictory consequences on the effects of doping on the visible-light photoactivities of titanium dioxide. Non-metals such as N, C and S (as an impurity) have also been studied for their visible light photocatalytic activities.[212–221] These studies informed that the non-metallic insertion enhanced photocatalytic actions as related to those for pure TiO_2 nanomaterials; particularly in the visible light region.[213] To obtain a charge balance, there are several procedures if an anion is substituted with a high valence anion. In TiO_2 lattice, nitrogen ions substitute oxygen atoms. Titanium dioxide nanotubes photocatalysts have been successfully prepared by Tokudome *et al.*[219] The author investigated breakdown of gaseous isopropanol into carbon dioxide and acetone by N-doped TiO_2 nanotubes. They observed that N-doped TiO_2 showed high photocatalytic oxidation activity when illuminated with visible light. Other points related to investigated photocatalytic activities of TiO_2 doped sulfur(s) have also been reported.[222] The results exhibited that in region of visible light S doped TiO_2 showed a high photocatalytic activity but lower in UV region. Recently, carbon has received significant interest as a nonmetallic dopant in TiO_2 materials. In visible light region, the decompositions of methylene blue and isopropanal have been demonstrated by C-doped TiO_2.[216] Using C-doped TiO_2 nanoparticles, Shen and colleagues[223] reported the degradation of trichloroacetic acid under visible light. They observed that C-doped titanium dioxide exhibited a remarkable photocatalytic activity for the reaction involved in degradation. Flouride doped TiO_2 was prepared by Yu *et al.*[224] The obtained F-TiO_2 displayed higher photocatalytic activity than undoped TiO_2 under proper preparation conditions.[224] For acetaldehyde and trichloroethylene decomposition, other comprehensive studies provided the investigated of N/F-doped TiO_2 nanomaterials. It was reported that TiO_2 nanomaterials (N/F-doped) had high visible light photocatalytic activities for decomposition reactions.[225,226] The different dopants moieties metal and nonmetal doping titanium dioxide and preparation procedures are given in Table 2. On the other hand, this table comprises splitting of water by photochemical cell reaction over numerous photo catalysts (Table 3).

4.2 Photovoltaic applications

Fig. 16 exhibits the principle of a dye sensitized solar cells (DSSC).[41] Dye sensitized solar cells have involved much consideration as reformative low priced substitutes to usual solid state devices.[227] A DSSC composed a nanoporous film

Table 2 The different dopants moieties metal and nonmetal-doping titanium dioxide and preparation methods

Kind of dopants	Doped elements	Preparation methods	Potential applications	Ref.
Metal dopants	Ag	Silver nitrate was mixed with reduction agent (sodium citrate tribasic dihydrate) and the reaction temperature was raised to 80 °C with continuous stirring. Then TIP and HNO_3 were added and the reaction was maintained at 50 °C for 24 h. The prepared sol was dried at 105 °C for 24 h and calcined at 300 °C	Degradation of nitrophenol in aqueous phase	316
	Fe	The reactive magnetron sputtering method: 99.99% titanium target and 99.9% iron pieces were placed in the reaction chamber and mixture of argon and oxygen was introduced into the chamber during discharging	Wastewater decoloring	317
	V	Sol–gel method: solution 1 (vanadyl acetylacetonate dissolved in *n*-butanol) was mixed with solution 2 (acetic acid in titanium butoxide) and hydrolyzed (24 h) by the water generated *via* the esterification of acetic and butanol. The suspension as dried at 150 °C, pulverized and calcined at 400 °C for 0, 5 h	Wastewater decoloring	318
	Au	Titanium(IV) butoxide dissolved in absolute ethanol was added to solution containing tetrachloroauric acid ($HAuCl_4 \cdot 4H_2O$), acetic acid and ethanol. The resulting suspension was aged (2 days), dried under vacuum, grinding and calcinated at 650 °C	Wastewater decoloring	319
	Pt	Photoreduction process: TiO_2 was suspended in a mixture of hexachloroplatinic acid in methanol. The suspension was irradiated with a 125 W mercury lamp (60 min). Pt–TiO_2 was separated by filtration, washed with distilled water and dried at 100 °C for 24 h	Wastewater decoloring	320
Nonmetal dopants	N	Titanium nitride (TiN) oxidation: Heating of TiN at 450–550 °C for 2 h in air (heating and cooling temperature rate: 2 °C min^{-1})	Photooxidation of aromatic compounds (*e.g.* toluene)	321
		Treating anatase TiO_2 powder ST01 in the NH_3	Photooxidation of acetaldehyde in gas phase	322

Table 2 (*Contd.*)

Kind of dopants	Doped elements	Preparation methods	Potential applications	Ref.
		(67%)/Ar atmosphere at 600 °C for 3 h		
	S	Oxidation annealing of titanium disulfide (TiS_2) at 300–600 °C	Wastewater decoloring	323
	N,S	Hydrolysis of $Ti(SO_4)_2$ in NH_3 aqueous solution. Precipitate was centrifuged, washed with distilled water and alcohol. Obtained gels were dried under vacuum at 80 for 10 h and were ground to obtain xerogel. The xerogel was calcinated at 400–800 °C in air for 3 h	Photooxidation of volatile compounds in gas phase (*e.g.* acetone and formaldehyde)	324
	C	Sol–gel method: TBOT was hydrolyzed in the presence of ethanol, water and nitric acid; precipitated titanium hydroxide was dried at 110 °C and calcinated in air at 150–200 °C	Photooxidation of phenol compounds in aqueous phase	325
		Acid-catalyzed sol–gel process. Alkoxidide precursor was dissolved in corresponding alcohol, mixed with hydrochloric acid aqueous solution. Obtained gel was aged for several days and calcinated in air (3 h at 65 °C and 3 h at 250 °C) and grounded	Photooxidation of phenol compounds in aqueous phase	326
	B	Anatase TiO_2 powder (ST01) was grinding with boric acid triethyl ester and calcinated in air at 450 °C	Improved photocatalytical activity	327
	P	Sol–gel method: TIP was hydrolyzed in the presence of isopropanol and water, after hydrolysis phosphoric acid was added. Dispersion was stirred for 2 h, centrifuged at 3500 rpm and dried at 100 °C. Obtained powder was calcinated at 300 °C	Photooxidation of phenol compounds in aqueous phase	328

prepared from mesoporous oxide layer of anatase TiO_2. Firstly, through a transparent conducting oxide (TCO) electrode, cell is illuminated where TiO_2 is deposited. Into the metal oxide conduction band, photo excited dye molecules insert electrons. I^-/IO_3^- couple acts as redox species in the electrolyte reducing the oxidized dye molecules back to their inventive state. Overall, the device produces electric power from light.[4,32] The surface of nanoporous TiO_2 film is bounded by more cations than the electrons. Henceforth, electron transport mechanism is measured to be purely diffusive.[228,229] From solid-state p–n junction, the process of absorption of light and the transport in the case of DSSCs are different due to distinct phenomenon. Through eqn (3) to (6), the process is described:

$$\text{Sensitizer (S)} + h\nu \rightarrow \text{S*(excited)} \quad (3)$$

$$\text{S*} + \text{TiO}_2 \rightarrow \text{e}^-(\text{TiO}_2) + \text{oxidized sensitizer}^+ \quad (4)$$

$$\text{Oxidized sensitizer}^+ + 3/2\ \text{I}^- \rightarrow \text{S} + 1/2\ \text{I}_3^- \quad (5)$$

$$1/2\ \text{I}_3^- + \text{e}^-(\text{counter electrode}) \rightarrow 3/2\ \text{I}^- \quad (6)$$

Table 3 Water splitting by photochemical–cell reaction over various photocatalysts

Photocatalysts	Weights	Reaction solutions	Light sources	Rate of evolutions (μmol h^{-1}) O_2	H_2	Ref.
Pt/TiO_2	0.3 g	2.17 M Na_2CO_3	400 W Hg lamp	568	287	329
ZrO_2	1 g	Distilled water	400 W Hg lamp	72	36	330
ZrO_2	1 g	1.09 M Na_2CO_3	400 W Hg lamp	142	75	330
Pt/ZrO_2	1 g	0.94 M $NaHCO_3$	400 W Hg lamp	120	61	330
Ru_2O/ZrO_2	1 g	Distilled water	400 W Hg lamp	11	5	330
Cu/ZrO_2	1 g	Distilled water	400 W Hg lamp	14	6	330
$NiO/Sr_2Nb_2O_7$	1 g	Distilled water	400 W Hg lamp	110	36	331
$NiO/Sr_2Ta_2O_7$	1 g	Distilled water	400 W Hg lamp	1000	480	331
(Tetra)$BaTa_2O_6$	1 g	Distilled water	400 W Hg lamp	21	10	332
(*Ortho*)$BaTa_2O_6$	1 g	Distilled water	400 W Hg lamp	33	15	332
(*Ortho*)$BaTa_2O_6$	1 g	0.0005 M $Ba(OH)_2$	400 W Hg lamp	126	59	332
(*Ortho*)$BaTa_2O_6$	1 g	0.001 M KOH	400 W Hg lamp	24	11	332
(*Ortho*)$BaTa_2O_6$	1 g	0.0005 M $BaCl_2$	400 W Hg lamp	15	6	332
$NiO/BaTa_2O_6$	1 g	Distilled water	400 W Hg lamp	629	303	332
$Ni/Rb_4Nb_6O_{17}$	1 g	Distilled water	400 W Hg lamp	936	451	333
$Ni/K_4Nb_6O_{17}$	1 g	Distilled water	400 W Hg lamp	403	197	333
Pt/TiO_2, TiO_2	12 mg	2 M KBr, 6.5 mM $FeCl_2$	500 W Hg	2.8	1.3	334
Pt–TaON, Pt–WO_3	0.2 g	5 mM NaI	300 W Xe lamp with filters: $\lambda > 420$ nm	24	12	335
$Pt/BaTaO_2N$, Pt/WO_3	0.1 g	5 mM NaI	300 W Xe lamp with filters: $\lambda > 420$ nm	6.6	3.1	336
$Pt/SrTiO_3$:Rh, $BiVO_4$	0.1 g	2 mM $FeCl_3$	300 W Xe with filter: $\lambda > 420$ nm	15	7.2	337
$Pt/SrTiO_3$:Rh, Bi_2MoO_6	0.1 g	2 mM $FeCl_3$	300 W Xe with filter: $\lambda > 420$ nm	19	8.9	235

From the equations, it is clear that photosensitizer (S) adsorbs light on the exterior of the semiconductor TiO_2 (eqn (3)). Then the photo-excited dye (S*) hand over electrons into titanium dioxide (eqn (4)). After that the reduced species found in the electrolyte (I^-) recovers electrons losing in the sensitizer (eqn (5)). Finally, by the mediator (I_3^-) that gains electrons (eqn (6)), the circuit is closed.

4.3 Photocatalytic water splitting

Photo-electrochemical and photo-catalytic water splitting to produce hydrogen are considered as potential procedures to achieve hydrogen. These are discussed below.

4.3.1 Fundamentals of photocatalytic water splitting. At semiconductor electrodes, breakdown of water is the main aim of lively research in current years. First, on a TiO_2 electrode, photocatalytic splitting of water was reported by Fujishima and Honda[4] in 1972. For green and sustainable energy sources,[230] photocatalytic water splitting into H_2 and O_2 using TiO_2 nanomaterials remains to be challenge. To drive chemical reactions, the generated electron and hole can be used. Water molecules for overall water splitting[231–233] are oxidized as well as reduced. The oxidation of water takes place by the holes to form O_2. While the reduction of water takes place by the electrons to form H_2. Of course, there are several features of TiO_2 but under solar energy, its photocatalytic water splitting efficacy is still quite low. Consequently, to activate the photocatalyst, only UV light can be utilized. It enhances its visible light response including upgraded bulk properties of the material. Water splitting mechanism on TiO_2 for hydrogen production is shown in Fig. 17.

4.3.2 Water splitting on TiO_2 nanotube arrays. TiO_2 nanotubes photocatalysts was investigated for water splitting under UV illumination by Shankar *et al.*[143] By potentiostatic anodization of titanium foil at 10 V in an electrolyte consist of (0.5% hydrofluoric acid, CH_3COOH mixed in a 7 : 1 ratio),[143] the TiO_2 nanotubes were prepared. Besides, four different electrolyte bath temperatures *i.e.* 5 °C, 25 °C, 35 °C, and 50 °C were tried to obtain the variation in the nanotubes length and thickness. TiO_2 nanotubes having pore diameter of 22 nm and wall thickness of 34 nm (ref. 156) were used to generate hydrogen gas. The total adaptation efficiency was 6.8%.[156] At 320–400 nm (98 mW cm^{-2}), the authors also reported that for illumination. The nanotube array of TiO_2 photoanodes may generate hydrogen from water with 12.25% photoconversion efficiency. On titanium foil; nanotube arrays with 570 nm in length and 70 nm in pore size; were prepared in 0.15 M hydrofluoric acid–0.5 M nitric acid by Xie *et al.*[217] Fig. 18 shows the comparison between the photoelectrochemical current of annealed TiO_2 nanotube array films and that of porous TiO_2. To higher surface area, the nanotube array samples with higher electrochemical current density were also ascribed.

4.3.3 Water splitting on doped TiO_2. Splitting of water has also been studied on TiO_2 obtained after doping with metal–non metals. Exactly doping is the incorporation of foreign elements into TiO_2 crystal lattice. The aim of doping is to enhance photocatalytic activities.[234] With the potential for H_2 evolution, certainly the band gaps of titanium dioxide semiconductor photocatalysts become extensive.

In a photoelectrochemical cell to oxidation and reduction of water to H_2 and O_2, Wrighton and colleagues[235] investigated the

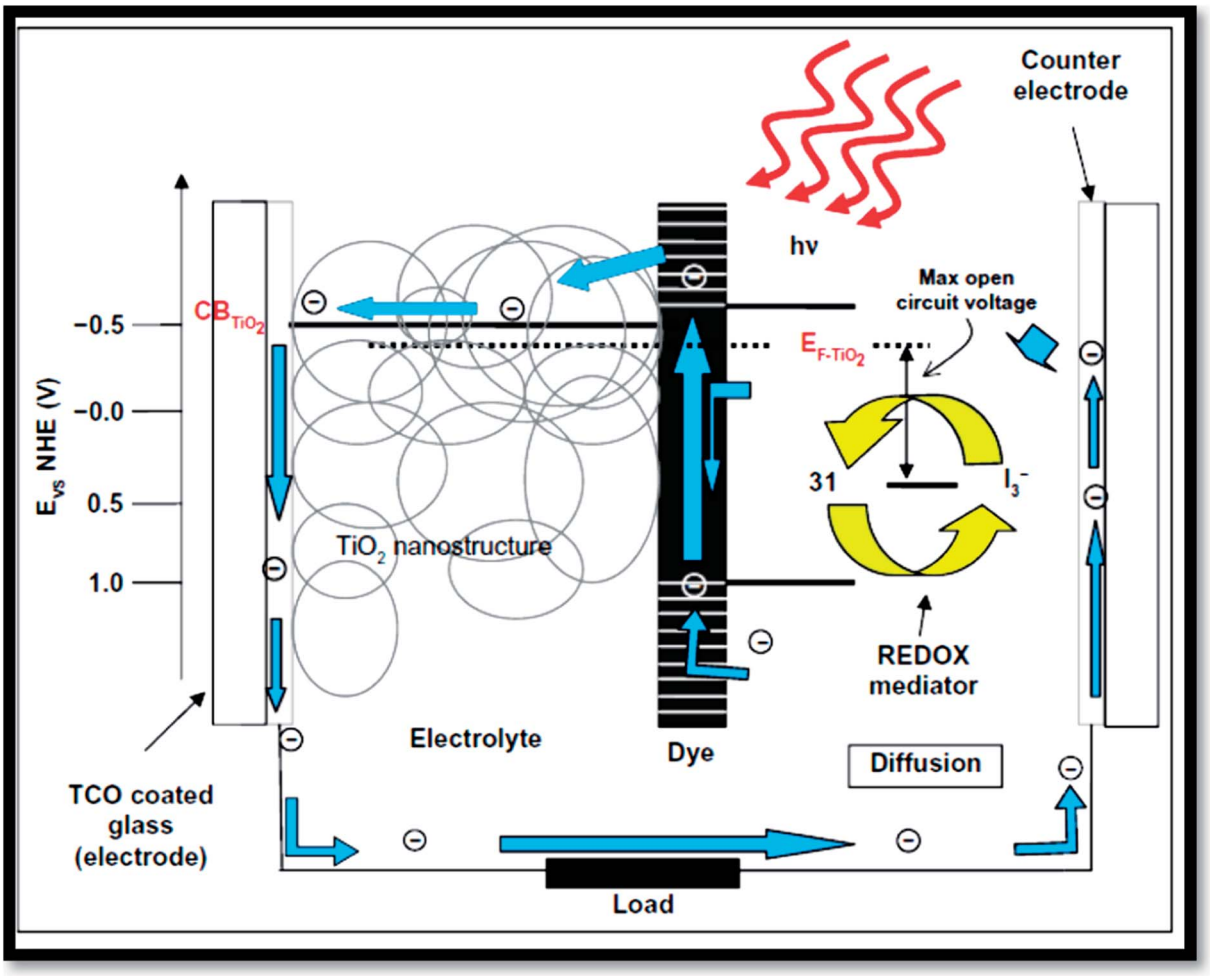

Fig. 16 Operation principles and energy levels of nanocrystalline dye-sensitized solar cell.[41]

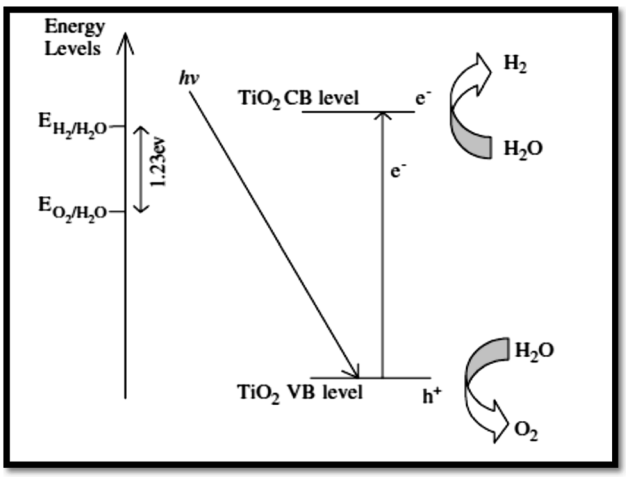

Fig. 17 Mechanism of TiO_2 photocatalytic water-splitting for hydrogen production.[230]

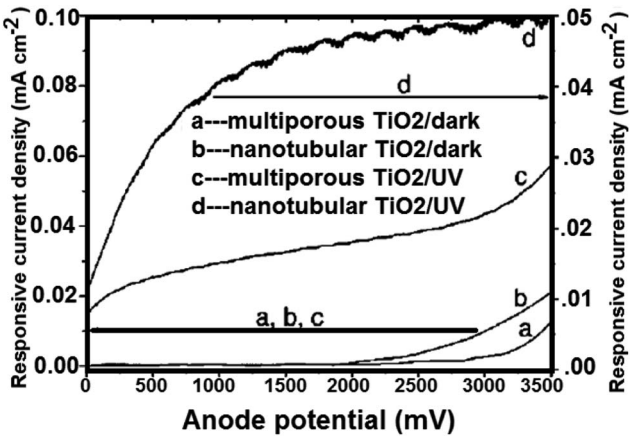

Fig. 18 Measured current of crystallized porous and nanotubular TiO_2/Ti electrodes under linearly swept potential from 0 to 3500 mV *vs.* SEC.[217]

use of an n-type semiconductor $SrTiO_3$ electrode. Without any external bias, decomposition of H_2O can be driven photochemically. Jin and co-workers[236] reported that TiO_2 doped with platinum/boron was a good system for splitting of water. Besides, Khan and colleagues[237] described the response for splitting of water on TiO_2 doped with carbon. The total conversion efficiency was 11%, which had a high water splitting

performance. The authors noted that at 40 mW cm^{-2} illumination, an extreme photo-conversion efficiency of 8.35% could be obtained. The synthesis of TiO_2 nanocrystalline thin films; with Pt-loaded through use of radio frequency magnetron sputtering method (RF); was described by Matsuoka *et al.*[238] They investigated that visible light was responsive for water decomposed in the occurrence of TiO_2 nanocrystalline.[239] Bocharov *et al.*[240] estimated theoretically the photocatalytic fitness of tinniest single wall fluorite structured titania (4,4) nanotube (NT) possessing three layers each (O–Ti–O) and doped by V, Ni, Mn, Sc, Cr, Fe, Co, Zn and Cu atoms substituted for host Ti atoms. They had associated electronic structure of ground state. For splitting of water, the results were in favor of Sc-doped titania nanotubes only for a potential photocatalytic usage. Using the sol–gel technique, Guayaquil *et al.*[241] synthesized a series of mesoporous TiO_2 (meso-TiO_2). At 500° and 550°, they were calcined following synthesis. For H generation, the mesoporous 2.50 wt% Pt–TiO_2 had the maximum photoactivity that was displayed by the prepared semiconductors. Alitabar *et al.*[242] increased the photocatalytic activity of TiO_2 nanotube arrays used as a photoanode in water splitting by doping it with sodium and carbon.

4.3.4 Water splitting on dye sensitized TiO_2. To increase the photocatalytic reaction efficiency, one of the ways is to couple TiO_2 semiconductor nanomaterials to an organic dye to employ visible light for energy change. Some dyes with visible light sensitivities can be utilized in photocatalytic systems and solar cells.[243–245] Duonghong and co-workers[246] studied the effect of using $Ru(bipy)_3^{2+}$ as a dye sensitizer under visible light radiation for hydrogen gas production. They reported water decomposition by using $[Ru(bipy)_3]^{2+}$ and rhodamine B under visible light. Besides, the effect of utilizing $[Ru(dcpy)_2(dpq)]^{2+}$ as a dye sensitizer, Alitabar and Yoozbashizadeh[242] carried out a parametric investigation on photocatalytic splitting of water for hydrogen gas manufacture under visible light irradiation. Hydrogen production was increased when dye molecules were adsorbed on to TiO_2. With the help of structure directing surfactant, Sreethawong *et al.*[247] prepared mesoporous-assembled TiO_2/Pt. Furthermore, the nitrogen doped TiO_2/Pt (N–TiO_2) was prepared *via* calcination of the hydrolysis product of $Ti(SO_4)_2$ with aqueous ammonia followed by platinum loading by Li *et al.*[248] N–TiO_2/Pt was sensitized and used for hydrogen production in occurrence of triethanolamine using anhydrous EtOH solution of eosin Y. Under comparable experimental conditions, it was observed that eosin Y–N–TiO_2/Pt exhibited advanced photocatalytic activity than eosin Y–TiO_2/Pt.

4.3.5 Water splitting on modified TiO_2. Many scientists have modified TiO_2 by different compounds to augment the process of water splitting. Over the surface of TiO_2, when silver oxide nano clusters were impregnated, Mandari *et al.*[249] synthesized plasmonic Ag_2O/TiO_2 photocatalysts. Zhang *et al.*[250] synthesized (g-C_3N_4) graphitic carbon nitride nanosheets/titanium dioxide (TiO_2) nanoparticles hetero-structure. The prepared g-C_3N_4/TiO_2 hetero-structured composites showed excellent photocatalytic hydrogen generation. Besides, on the g-C_3N_4 nanosheets the TiO_2 nanoparticles were well dispersed. The as obtained g-C_3N_4 coupled with TiO_2 not only increased the surface area of g-C_3N_4, but also promoted the separation of photo-generated charge carriers. Hou *et al.*[251] used two typed gold films (i) coated with TiO_2 (ii) and uncoated with TiO_2. After that, they reported measurements of photocatalytic water splitting. For hydrogen gas production with Pt and CoO_x as dual cocatalysts, Zhang *et al.*[252] reported a new CoO_x/TiO_2/Pt photocatalyst. This type of catalyst was prepared by template assisted atomic layer deposition (ALD). Under UV light irradiation, the generated electrons and holes transfer to the different surfaces of TiO_2 nanotubes. Photocatalytic efficiency of CoO_x/TiO_2/Pt photocatalysts was 275.9 μmol h^{-1}, while that pristine TiO_2 nanotubes was 56.5 μmol h^{-1}. Xu *et al.*[253] synthesized novel plate like $Co(OH)_2$ decorated TiO_2 nanosheets for photocatalytic hydrogen generation illustrating $Co(OH)_2$ decorated TiO_2 samples of high rate of hydrogen generation than native TiO_2 sample. Sui *et al.*[254] prepared a Pt/TiO_2 catalyst, where Pt was atomically and selectively dispersed on the (1 0 1) facets of nanosized TiO_2 single crystals. For H_2 production, a remarkably higher photocatalytic activity was compared to frequently used Pt/TiO_2. Si *et al.*[255] synthesized anatase TiO_2, thin TiO_2 (B) nanosheets and their composites. The properly aligned structure of band, with the conduction band level of ultra-thin TiO_2 (B) was about 0.6 eV higher than that of the anatase. Wang *et al.*[256] reported that very small amount of fluorine inhibited hydrogen and oxygen recombination. The detailed study showed that inhibition was by occupation of hydrogen and oxygen sorption and activation sites by fluorine ion over platinum. Liu *et al.*[257] fabricated a composite photoanode having TiO_2 nanotube arrays altered with polyoxometalate (POM) and Co_9S_8.

5. Mechanism of water splitting

On surface modification of TiO_2, a number of efforts have been made to expand the photocatalytic activities as simple change can eagerly adjust the mechanisms and accelerates the kinetics of photocatalysis.[258,259] In the UV regime, the band gap for TiO_2 lies. Besides, the latter has lower photocatalytic activities due to the lower ECB of ritual by ~0.2 eV. For modification of TiO_2 nanomaterials, the goals are to improve their optical activities.[213,214] There are several methods to recover the performance of TiO_2 nanomaterials. In visible light, other colorful compounds sensitizing TiO_2 might be improved optical activity. Second, doping with other elements can also change the optical properties of TiO_2 nanomaterials. At the atomic level, Hussain *et al.*[260] explored the interfacial structure between a rutile TiO_2(110) surface pre-characterized and liquid water. The mechanism of splitting of water occurring in the occurrence of semiconductor photocatalyst was explained by Salvador in 1–4 equations as follows.[261]

$$\text{Semiconductor} + 2h\nu \rightarrow 2h^+ + 2e^-$$

$$H_2O + 2h^+ \rightarrow \frac{1}{2}O_2 + 2H^+ \left(E_{O_2/H_2O}\right)$$

$$2H^+ + 2e^- \rightarrow H_2(E_{H_2O/H_2})$$

$$H_2O \xrightarrow{h\nu} H_2(g) + \frac{1}{2}O_2(g)$$

EtOH serves as a sacrificial reagent which also helps to increase the entire process efficiency.[64] Water splitting mechanism on Ag/TiO_2 was explained by Liu *et al.*[262]

According to Salvador *et al.*[261] during the process of water splitting, formation of H^+ and OH^- can take place through the reaction of H_2O molecules with holes in TiO_2 valence band. The consumption of ·OH can occur through chemical reaction with CH_3CH_2OH. With enhanced energy, the electrons react with H^+ at the surface of Ag NPs where H^+ can take an electron through SPR (surface plasmon resonance) to generate an H atom, and then 2H atoms associate with each other for the formation of an H_2 molecule.

$$TiO_2 + h\nu \rightarrow h_{vb}^+ + e_{cb}^-$$

$$e_{cb}^- \rightarrow e_{Ag}^-$$

$$e_{Ag}^- + h\nu(\text{visible}) \rightarrow e_{SPR}^-$$

$$h_{vb}^+ + H_2O \rightarrow \cdot OH + H^+$$

$$CH_3CH_2OH + \cdot OH \rightarrow CH_3COOH + H^+$$

$$e_{SPR}^- + H^+ \rightarrow H$$

$$H + H \rightarrow H_2$$

With an I^-/IO_3^- (iodide/iodate) redox-mediator system, water splitting mechanism on TiO_2 was explained by Nishijima *et al.*[263] Besides, they studied the photoassisted oxidation of water continued with impartially high efficiency when Fe^{3+} ions were used as electron acceptors. This whole process of splitting of water on doped titanium dioxide; containing a rutile phase; was compared to that on doped titanium dioxide with an anatase phase. After all, they proposed the mechanism of water splitting in following equations:

$$TiO_2 + h\nu \rightarrow e^- + h^+$$

$$2H_2O + 4h^+ \rightarrow O_2 + 4H^+$$

$$Fe^{3+} + e^- \rightarrow Fe^{2+}$$

$$C_2H_5OH + 3H_2O + 6h^+ \rightarrow 2CO_2 + 6H^+$$

$$2H^+ + 2e^- \rightarrow H_2$$

$$4OH^- + 4h^+ \rightarrow O_2 + 2H_2O$$

$$IO_3^- + 3H_2O + 6e^- \rightarrow I^- + 6OH^-$$

$$2H_2O + 2e^- \rightarrow H_2 + 2OH^-$$

$$I^- + 6OH^- + 6h^+ \rightarrow IO_3^- + 3H_2O$$

Mechanism for water splitting on TiO_2 photosensitized by glutathione capped metal nanoclusters was explained by Chen and Kamat.[264] In aqueous buffer solution (pH = 7), a mesoscopic TiO_2 film photosensitized by glutathione capped metal nanoclusters (Aux-GSH NCs) was utilized as the photoanode with platinum counter electrode. After all, they also proposed the water splitting mechanism as follows:

$$Au_x - GSH \xrightarrow{h\nu} Au_x - GSH^*$$

$$Au_x - GSH^* \cdots TiO_2 \rightarrow Au_x - GSH^+ \cdots TiO_2(e)$$

$$TiO_2(e) + Pt \rightarrow TiO_2 + Pt(e)$$

$$Pt(e) + H^+ \rightarrow 1/2H_2$$

$$Au_x - GSH^+ + 1/2H_2O \rightarrow Au_x - GSH + 1/4O_2 + H^+$$

$$Au_x - GSH^+ \xrightarrow{\text{accumulated holes}} Au_x - GSH^{y+}$$

$$Au_x - GSH^+ + EDTA \rightarrow Au_x - GSH + \text{oxidized EDTA}$$

6. Lithium batteries

As the most promising energy storage technologies, lithium ion batteries (LIBs) are measured as the best for renewable energy, electric vehicles and mobile electronics. In recent years, as a possible anode, TiO_2 (B) has received growing interest for Li ion batteries. As compared to commercialized $Li_4Ti_5O_{12}$, it offers higher energy storage. From the micron to the nanoscale, it is better than rutile and anatase. The important factors playing an important role and greatly affect the lithium ion batteries (LIB) performance are particle size and crystallographic alignment of the nanostructured.[265–267] The crystallographic orientations [such as TiO_2(B)] and the theoretical studies[268,269] confirmed that lithium ion mobility favors the direction in the order of $b > c >> a$-axis channel.[270]

7. Gas sensors

The other application of TiO_2 nanocrystalline is as gas sensor because gas adsorption causes a change in electrical conductivity like ZnO semiconductors.[155,270–272] Thus, TiO_2 is usually used as an oxygen gas instrument, *e.g.* to gauge the burning process of fuel in car engines to control fuel environmental pollution and consumption. Grimes *et al.*[155] considered the use of titanium dioxide as sensor.

8. White pigments

The pigment being the most abundant component in the coating affects the properties of the coating materials. Because of its highest refractive index of stability, colorless, and relatively low and uniform absorption of visible light, titanium dioxide has newly become a core white pigment source of scattering of light. By two procedures *i.e.* hydrothermal and hydrolysis, Samya El-Sherbiny *et al.*[273] created anatase and rutile. In paper coating, the usage of the prepared nano-pigments disclosed that a slight amount of titanium dioxide was satisfactory to attain important improvements in brightness and opacity. It is due to ability of scattering light.

9. TiO_2-based nanocomposites as catalysts

TiO_2 photo catalysts have been widely studied for the uptake of organic contaminants in water and air.[274] The present article also concentrated on hybrid nanocrystals based on TiO_2, describing different examples of synthetic methods and deliberating their applications in water treatment. Some papers are reported in the area of hybrid nanocrystals preparation. The papers on the photocatalytic features of nanocatalysts indicated their huge measure applications as challenges. However, these nanomaterials hold good assurance for the dilapidation of organic and inorganic contaminants in water or gas phase. The main features of nano sized TiO_2 materials are enormously high surface to volume ratio and turning into a great density of catalytically surface sites.[275] The another fact is the size reliant band gap of nano sized semiconductors. It is likely to finely adjust the redox potentials of photogenerated electron hole couples to selectively control photochemical reactions. Besides, the catalyst surface is occupied easily by charges photogenerated in nano-catalysts.[276] The hybrid nanocrystals formed by two or more components hold great promise for the development of multifunctional nanocatalysts among the embarrassment of methods proposed in the literature so far.[277–281] Indeed, the opportunity is offered by hybrid nanocrystals to merge in one material resulting in countless possible combinations.[282–285] Under visible light irradiation, spatial separation of e^-/h^+ could also be provide by the photoactivity hybrid nanocrystals. Thus, improving is an occasion to magnetically recuperate the photocatalysts or stimulate biocidal utility even in the dark. The surface properties, the particle size of the catalysts, their morphology, the composition, organization of the metal and TiO_2 are the factors, which also affect the photocatalytic efficiency.[286] Therefore, for the preparation of metal nanoparticle hybrid hetero-structures, numerous synthetic methods have been described, which include impregnation,[287] UV irradiation,[288] electrodeposition,[289] sonochemistry,[290] hydrothermal,[291] sol–gel,[292] and flame-spray synthesis.[293] Wenqing *et al.*[294] prepared nanocomposites of titanium dioxide (P25) and reduced graphene oxide (RGO) utilizing numerous methods such as hydrazine reduction, UV-assisted photocatalytic reduction and hydrothermal. Those nanocomposites were studied as photocatalysts for the progress of hydrogen from alcohol solution under UV-vis irradiation. It was found that the assimilation of RGO into P25 considerably increased the photocatalytic activity for H_2 evolution, and the P25–RGO composite synthesized by the hydrothermal method showed the excellent presentation. Deepa *et al.*[295] prepared Au/TiO_2 nanocomposites for photocatalytic hydrogen generation in the company of a sacrificial electron donor like ethanol or methanol under UV-visible and visible light irradiation. These nanocomposites exhibited excellent photocatalytic activity for hydrogen generation under UV-visible conditions. Amount of hydrogen evolved using Au/TiO_2 nanocomposites under dark condition was zero. Anna and Jerzy[296] studied the hydrogen generation by water splitting on Pt–TiO_2 catalyst. Besides, they also examine the influence of numerous sacrificial chemicals like MeOH, Na_2S, and ethylene diamine tetraacetic acid (EDTA), I^- and IO_3^- ions on the photocatalytic efficacy in water splitting reactions in ultraviolet (UV) illumination. Photocatalytic water splitting was achieved at EDTA and Na_2S utilization as the sacrificial reagents. Yatskiv *et al.*[297] reported that the photocatalytic systems having mesoporous TiO_2 and Pd/SiO_2, produced extra quantities of molecular hydrogen at keeping in dark after the ending of irradiation. Václav and Daniela[298] prepared TiO_2/ZnS/CdS composites by homogeneous hydrolysis of aqueous solutions mixture of TiO_2SO_4, $ZnSO_4$, and $CdSO_4$ with thioacetamide for photocatalytic hydrogen production from water. Hydrogen generation was seen in the company of Pd and Pt nanoparticles deposited on TiO_2/ZnS/CdS composites. The excellent photocatalytic activity for H_2 evolution indicated with $TiZnCd_7$ on surface deposited with palladium, which had 78.5% ZnS, 20.21% TiO_2, and 1.29% CdS·TiO_2/ZnS/CdS. Quanjun *et al.*[299] reported new composite material having of TiO_2 nanocrystals *via* two steps hydrothermal process utilizing thiourea, sodium molybdate and graphene oxide as precursors with tetrabutylorthotitanate and MoS_2/graphene hybrid as titanium precursors. TiO_2/MoS_2/graphene composite attained high H_2 generation rate of 165.3 μmol h^{-1} without a noble metal co-catalyst. Anna *et al.*[300] interpreted the development of the quantum yield of H_2 generation using TiO_2/Ag^0 to TiO_2/Ni^0 to TiO_2/Cu^0 in terms of alterations in the electronic interface between the semiconductor surface and metal nanoparticles. They observed a controlled metal amount range for maximum quantum yield of hydrogen generation. Ke *et al.*[301] examined Pt-loaded nanocomposites, pristine MWNTs and TiO_2 for their photocatalytic activities for water splitting with triethanolamine as an electron donor. Hydrogen was effectively generated on Pt/MWNT–TiO_2 in visible light illumination ($\lambda > 420$ nm). Hydrogen production rate up to 8 mmol g^{-1} h^{-1} under full spectral irradiation of a Xe-lamp, or more was attained. Takuya *et al.*[302] investigated the photocatalytic hydrogen generation in $MeOH_n$ with CuO/TiO_2, SnO/TiO_2, ZnO/TiO_2, CuO/Al_2O_3/TiO_2 and Al_2O_3/TiO_2 nanocomposites. The maximum hydrogen generation was achieved with CuO/Al_2O_3/TiO_2 nanocomposites having 0.3 wt% Al_2O_3/TiO_2/0.2 wt% CuO. Nitish *et al.*[303] demonstrated the higher hydrogen evolution reaction (HER) activity of Pt nanoparticles (Pt NPs) reinforced on titanium dioxide (TiO_2) nanocrystals (Pt–TiO_2) and nitrogen doped

reduced graphene oxide (N-rGO) constructed TiO_2 nanocomposite (Pt–TiO_2–N-rGO). Lu *et al.*[304] prepared TiO_2 photocatalysts with nickel sulfide co-catalyst by stocking nickel sulfide on TiO_2 with solvothermal synthesis method. It was reported that NiS was used as a co-catalyst with TiO_2 for the photocatalytic generation of H_2. High hydrogen generation was achieved with NiS as hexagonal structure with content in the composite of 7 at% in relation to TiO_2. The rate of H_2 generation was augmented by 30 times than that of TiO_2 alone. Fuyun *et al.*[305] prepared nanocomposite of N-doped TiO_2 with graphene oxide (NTG) to improve the photocatalytic efficiency. NTG exhibited high photocatalytic efficiency hydrogen evolution. It was of 716.0 or 112.0 μmol h^{-1} g^{-1} at high pressure Hg or Xe lamp, which was around 9.2 or 13.6 times higher than P25 photocatalyst.

Recently, gold nanoparticles were reinforced on TiO_2–C_3N_4 for CO oxidation in visible light illumination exploiting hydrothermal method; beginning with titanium glycolate and graphitic C as precursors. TiO_2–C_3N_4 microspheres were prepared and then decorated with gold nanoparticles by letting HAuCl reaction at alkaline pH (pH = 10) in the attendance of sodium carbonate. After 2 h, the dried and washed powder was calcinated at 350 °C.[306] Besides, visible light dynamic silver modified titania catalyst was described for the utilization in the decomposition of MeOH, CH_3COOH, 2-PrOH and *Escherichia coli*.[307] A plasmonic gold silver alloy on TiO_2 photocatalyst was also described that indicated elevated degradation of stearic acid at 490 nm than reported using pristine TiO_2.[308]. Qiu *et al.*[309] have described that Cu_xO/TiO_2 photocatalyst resulted into effective VOCs uptake. Furthermore, Wang *et al.*[310] prepared and used TiO_2 NRs/Fe_xO_y/Ag core shell nanostructures for photodegradation of rhodamine B in solar light illumination. Recently, a reviews described successful removal of benzene, methylene blue and carbamazepine by photodegradation using CNT/TiO_2 nanostructured composites.[311]

10. Future challenges and perspectives

Recently, the applications of TiO_2 nanostructures have been exploited to clean environment and produce hydrogen. But there are certain limitations, which we have to overcome to make the structures applicable in real life problems. The efficiencies of these structures are not excellent; especially for decomposing of persistent organic volatile pollutants and production of hydrogen at large scale. Generally, doped TiO_2 nanostructures result into poor photoactivity. Other challenges are to augment spectral sensitivity of these structures to visible and NIR regions and the bio-compatibility of TiO_2 nanostructures. Therefore, there is a great need of future research focusing constant photoactivity in the long run. These can be achieved by modifying the synthetic routs. Nonmetal doped TiO_2 nanostructures have low photocatalytic activity under visible light UV radiation. Therefore, some materials such as polymers, glass, ceramics, or metals may serve as magical identities in this area for economic and eco-friendly applications.

Future research needs the development of new synthetic procedures and nanostructures with higher surface states. It may be served by non-lithographic complementary metal oxide semiconductor compatible techniques. This technique may be applicable for new doping materials, dopant incorporation into TiO_2 nanostructures and applications for environmental and alternate energy areas. Besides, visible to near infra-red activated titanium nanostructures should be designed. TiO_2 nanostructures may serve as the ideal materials in biological and medicinal science. Therefore, there is a great need to study the bio-compatibility of these structures at supra molecular level. In a nut shell, the researchers have several challenges to tackle with them in near future. Therefore, there is a great need to improve the structures and properties of these materials. The basic knowledge of chemistry, physics and computer modeling may help to achieve the task.

11. Conclusion

An inclusive review of the syntheses, properties and applications of TiO_2 nanostructures is offered. These nanostructures can be prepared by different synthesis procedures as per the requirements. It was observed that the physico-chemical properties of titanium dioxide nanostructures are responsible for wide applications in several fields such as gas sensors, white pigments, lithium batteries, photocatalytic applications (photodegradation of organic compounds), photovoltaic applications and water splitting. TiO_2 nanostructures play a great role in water purification by degrading biological and organic pollutants. The use in generating hydrogen as a green currency is the biggest asset of nano TiO_2 structures. It was observed that the decomposing and water splitting properties of TiO_2 nanostructures are not good enough, which can be exploited at a commercial level economically. It may be predicted that these materials may be the choice in water purification. Most interestingly, we believe that TiO_2 nanostructures will achieve a great reputation in generation of hydrogen fuel – a need of the next century.

Conflicts of interest

There is no conflict of interest.

References

1 G. Pfaff and P. Reynders, *Chem. Rev.*, 1999, **99**, 1963–1982.
2 A. Salvador, M. C. Pascual-Martí, J. R. Adell, A. Requeni and J. G. March, *J. Pharm. Biomed. Anal.*, 2000, **22**, 301–306.
3 M. D. Newman, M. Stotland and J. I. Ellis, *J. Am. Acad. Dermatol.*, 2009, **61**, 685–692.
4 A. Fujishima and K. Honda, *Nature*, 1972, **238**, 37–38.
5 T. Kaida, K. Kobayashi, M. Adachi and F. Suzuki, *J. Cosmet. Sci.*, 2004, **55**, 219–220.
6 J. J. Wang, B. J. S. Sanderson and H. Wang, *Mutat. Res., Genet. Toxicol. Environ. Mutagen.*, 2007, **628**, 99–106.

7 R. A. Schwartz, *Acta Dermatovenerol. Croat.*, 2004, **12**(4), 249.
8 J. J. Jacobs, A. K. Skipor, J. Black, R. M. Urban and J. O. Galante, *J. Bone Jt. Surg., Am. Vol.*, 1991, **73**, 1475–1486.
9 Y. Sul, *Int. J. Nanomed.*, 2010, **5**, 87–100.
10 A. Patri, T. Umbreit, J. Zheng, K. Nagashima, P. Goering, S. Francke-Carroll, E. Gordon, J. Weaver, T. Miller, N. Sadrieh, S. McNeil and M. Stratmeyer, *J. Appl. Toxicol.*, 2009, **29**, 662–672.
11 A. Fujishima, T. N. Rao and D. A. Tryk, *J. Photochem. Photobiol., C*, 2000, **1**, 1–21.
12 D. Tryk, A. Fujishima and K. Honda, *Electrochim. Acta*, 2000, **45**, 2363–2376.
13 M. Gratzel, *J. Sol-Gel Sci. Technol.*, 2001, **22**, 7–13.
14 S. Ivanković, M. Gotić, M. Jurin and S. Musić, *J. Sol-Gel Sci. Technol.*, 2003, **27**, 225–233.
15 A. L. Linsebigler, G. Lu and J. T. Yates, *Chem. Rev.*, 1995, **95**, 735–758.
16 A. Mills and S. Le Hunte, *J. Photochem. Photobiol., A*, 1997, **108**, 1–35.
17 A. P. Alivisatos, *J. Phys. Chem.*, 1996, **100**, 13226–13239.
18 A. Hagfeldt and M. Graetzel, *Chem. Rev.*, 1995, **95**, 49–68.
19 A. P. Alivisatos, *Science*, 1996, **271**, 933–937.
20 C. Burda, X. Chen, R. Narayanan and M. A. El-Sayed, *Chem. Rev.*, 2005, **105**, 1025–1102.
21 C. B. Murray, C. R. Kagan and M. G. Bawendi, *Annu. Rev. Mater. Sci.*, 2000, **30**, 545–610.
22 Y. Yin and A. P. Alivisatos, *Nature*, 2005, **437**, 664–670.
23 D. M. Adams, L. Brus, C. E. D. Chidsey, S. Creager, C. Creutz, C. R. Kagan, P. V. Kamat, M. Lieberman, S. Lindsay, R. A. Marcus, R. M. Metzger, M. E. Michel-Beyerle, J. R. Miller, M. D. Newton, D. R. Rolison, O. Sankey, K. S. Schanze, J. Yardley and X. Zhu, *J. Phys. Chem. B*, 2003, **107**, 6668–6697.
24 D. Beydoun, R. Amal, G. Low and S. McEvoy, *J. Nanopart. Res.*, 1999, **1**, 439–458.
25 X. Chen, Y. Lou, S. Dayal, X. Qiu, R. Krolicki, C. Burda, C. Zhao and J. Becker, *J. Nanosci. Nanotechnol.*, 2005, **5**, 1408–1420.
26 H. Dai, *Acc. Chem. Res.*, 2002, **35**, 1035–1044.
27 M. S. Dresselhaus and G. Dresslhaus, *Annu. Rev. Mater. Sci.*, 1995, **25**, 487–523.
28 M. S. Dresselhaus, G. Dresselhaus, A. Jorio, A. G. Souza Filho, M. A. Pimenta and R. Saito, *Acc. Chem. Res.*, 2002, **35**, 1070–1078.
29 M. S. Dresselhaus, G. Dresselhaus and A. Jorio, *Annu. Rev. Mater. Res.*, 2004, **34**, 247–278.
30 A. L. Efros and M. Rosen, *Annu. Rev. Mater. Sci.*, 2000, **30**, 475–521.
31 M. A. El-Sayed, *Acc. Chem. Res.*, 2004, **37**, 326–333.
32 M. Gratzel, *Prog. Photovoltaics*, 2000, **8**, 171–185.
33 M. R. Hoffmann, S. T. Martin, W. Choi and D. W. Bahnemann, *Chem. Rev.*, 1995, **95**, 69–96.
34 S. Link and M. A. El-Sayed, *Annu. Rev. Phys. Chem.*, 2003, **54**, 331–366.
35 S. S. Mao, *Int. J. Nanotechnol.*, 2004, **1**, 42.
36 M. Nirmal and L. Brus, *Acc. Chem. Res.*, 1999, **32**, 407–414.
37 A. J. Nozik, *Inorg. Chem.*, 2005, **44**, 6893–6899.
38 A. J. Nozik, *Annu. Rev. Phys. Chem.*, 2001, **52**, 193–231.
39 M. Ouyang, J.-L. Huang and C. M. Lieber, *Acc. Chem. Res.*, 2002, **35**, 1018–1025.
40 L. Vayssieres, *Int. J. Nanotechnol.*, 2004, **1**(1–2), 1–41.
41 M. Grätzel, *J. Photochem. Photobiol., C*, 2003, **4**, 145–153.
42 V. E. Henrich, *Rep. Prog. Phys.*, 1985, **48**, 1481–1541.
43 J. F. Banfield, B. L. Bischoff and M. A. Anderson, *Chem. Geol.*, 1993, **110**, 211–231.
44 P. Y. Simons and F. Dachille, *Acta Crystallogr.*, 1967, **23**, 334–336.
45 J. Tang and S. Endo, *J. Am. Ceram. Soc.*, 1993, **76**, 796–798.
46 J. S. Olsen, L. Gerward and J. Jiang, *J. Phys. Chem. Solids*, 1999, **60**, 229–233.
47 M. Latroche, L. Brohan, R. Marchand and M. Tournoux, *J. Solid State Chem.*, 1989, **81**, 78–82.
48 J. Akimoto, Y. Gotoh, Y. Oosawa, N. Nonose, T. Kumagai, K. Aoki and H. Takei, *J. Solid State Chem.*, 1994, **113**, 27–36.
49 R. Marchand, L. Brohan and M. Tournoux, *Mater. Res. Bull.*, 1980, **15**, 1129–1133.
50 J. Haines and J. M. Léger, *Phys. B*, 1993, **192**, 233–237.
51 M. Horn, C. F. Schwebdtfeger and E. P. Meagher, *Z. Kristallogr. Cryst. Mater.*, 1972, **136**, 273–281.
52 W. H. Baur, *Acta Crystallogr.*, 1961, **14**, 214–216.
53 S.-D. Mo and W. Y. Ching, *Phys. Rev. B: Condens. Matter Mater. Phys.*, 1995, **51**, 13023–13032.
54 J. Pascual, J. Camassel and H. Mathieu, *Phys. Rev. B: Condens. Matter Mater. Phys.*, 1978, **18**, 5606–5614.
55 A. Eucken and A. Büchner, *Z. Phys. Chem.*, 1934, **27B**, 321–349.
56 G. E. Jellison, F. A. Modine and L. A. Boatner, *Opt. Lett.*, 1997, **22**, 1808.
57 N. Hosaka, T. Sekiya, C. Satoko and S. Kurita, *J. Phys. Soc. Jpn*, 1997, **66**, 877–880.
58 D. C. Cronemeyer, *Phys. Rev.*, 1952, **87**, 876–886.
59 L. Forro, O. Chauvet, D. Emin, L. Zuppiroli, H. Berger and F. Lévy, *J. Appl. Phys.*, 1994, **75**, 633–635.
60 R. R. Hasiguti and E. Yagi, *Phys. Rev. B: Condens. Matter Mater. Phys.*, 1994, **49**, 7251–7256.
61 G. A. Acket and J. Volger, *Physica*, 1966, **32**, 1680–1692.
62 R. G. Breckenridge and W. R. Hosler, *Phys. Rev.*, 1953, **91**, 793–802.
63 H. P. R. Frederikse, *J. Appl. Phys.*, 1961, **32**, 2211–2215.
64 X. Chen and S. S. Mao, *Chem. Rev.*, 2007, **107**, 2891–2959.
65 T. L. Thompson and J. T. Yates, *Chem. Rev.*, 2006, **106**, 4428–4453.
66 U. Diebold, *Surf. Sci. Rep.*, 2003, **48**, 53–229.
67 A. Navrotsky, J. C. Jamieson and O. J. Kleppa, *Science*, 1967, **158**, 388–389.
68 Q. Zhang, *Appl. Catal., B*, 2000, **26**, 207–215.
69 L. Thiên-Nga and A. T. Paxton, *Phys. Rev. B: Condens. Matter Mater. Phys.*, 1998, **58**, 13233–13241.
70 G. Cangiani, Ab-initio Study of the Properties of TiO2 Rutile and Anatase Polytypes, PhD thesis, EPFL – Environmental Chemistry Modeling Laboratory, SISSA, Trieste, Italy, 2003.
71 J. Muscat, V. Swamy and N. M. Harrison, *Phys. Rev. B: Condens. Matter Mater. Phys.*, 2002, **65**, 224112.

72 A. Di Paola, M. Addamo, M. Bellardita, E. Cazzanelli and L. Palmisano, *Thin Solid Films*, 2007, **515**, 3527–3529.
73 N. Liu, H. G. Steinrück, A. Osvet, Y. Yang and P. Schmuki, *Appl. Phys. Lett.*, 2017, **110**, 072102-1–072102-4.
74 J. Jamieson and B. Olinger, *Miner Notes*, 1969, **54**, 1477.
75 F. Bregani, C. Casale, L. E. Depero, I. Natali-Sora, D. Robba, L. Sangaletti and G. P. Toledo, *Sens. Actuators, B*, 1996, **31**, 25–28.
76 M. E. Straumanis, T. Ejima and W. J. James, *Acta Crystallogr.*, 1961, **14**, 493–497.
77 O. R. S. da Rocha, R. F. Dantas, M. M. M. B. Duarte, M. M. L. Duarte and V. L. da Silva, *Chem. Eng. J.*, 2010, **157**, 80–85.
78 G. K. Mor, O. K. Varghese, M. Paulose, K. Shankar and C. A. Grimes, *Sol. Energy Mater. Sol. Cells*, 2006, **90**, 2011–2075.
79 Y. Ao, J. Xu, S. Zhang and D. Fu, *Appl. Surf. Sci.*, 2010, **256**, 2754–2758.
80 L. Dong, G. Cao, Y. Ma, X. Jia, G. Ye and S. Guan, *Trans. Nonferrous Met. Soc. China*, 2009, **19**, 1583–1587.
81 S. Banerjee, J. G. Pal, P. Muraleedharan, A. K. Tyagi and B. Raj, *Res. Commun.*, 2006, **90**, 1378–1383.
82 S. Sakthivel and H. Kisch, *Angew. Chem., Int. Ed.*, 2003, **42**, 4908–4911.
83 H. K. Ardakani, *Thin Solid Films*, 1994, **248**, 234–239.
84 A. T. Paxton and L. Thiên-Nga, *Phys. Rev. B: Condens. Matter Mater. Phys.*, 1998, **57**, 1579–1584.
85 E. C. Akubuiro and X. E. Verykios, *J. Phys. Chem. Solids*, 1989, **50**, 17–26.
86 S. Fujitsu and T. Hamada, *J. Am. Ceram. Soc.*, 1994, **77**, 3281–3283.
87 N. G. Eror, *J. Solid State Chem.*, 1981, **38**, 281–287.
88 J.-L. Carpentier, A. Lebrun and F. Perdu, *J. Phys. Chem. Solids*, 1989, **50**, 145–151.
89 P. Knauth and H. L. Tuller, *J. Appl. Phys.*, 1999, **85**, 897–902.
90 K. Mizushima, M. Tanaka, A. Asai, S. Iida and J. B. Goodenough, *J. Phys. Chem. Solids*, 1979, **40**, 1129–1140.
91 N. Yu and J. W. Halley, *Phys. Rev. B: Condens. Matter Mater. Phys.*, 1995, **51**, 4768–4776.
92 H. X. Zhu, P. X. Zhou, X. Li and J.-M. Liu, *Phys. Lett. A*, 2014, **378**, 2719–2724.
93 F. Arntz and Y. Yacoby, *Phys. Rev. Lett.*, 1966, **17**, 857–860.
94 A. Frova, P. J. Boddy and Y. S. Chen, *Phys. Rev.*, 1967, **157**, 700–708.
95 A. K. Ghosh, F. G. Wakim and R. R. Addiss, *Phys. Rev.*, 1969, **184**, 979–988.
96 A. Amtout and R. Leonelli, *Phys. Rev. B: Condens. Matter Mater. Phys.*, 1995, **51**, 6842–6851.
97 S. Hüfner and G. K. Wertheim, *Phys. Rev. B: Solid State*, 1973, **7**, 2333–2336.
98 D. W. Fischer, *Phys. Rev. B: Condens. Matter Mater. Phys.*, 1972, **5**, 4219–4226.
99 F. M. F. de Groot, J. Faber, J. J. M. Michiels, M. T. Czyżyk, M. Abbate and J. C. Fuggle, *Phys. Rev. B: Condens. Matter Mater. Phys.*, 1993, **48**, 2074–2080.
100 L. A. Grunes, *Phys. Rev. B: Condens. Matter Mater. Phys.*, 1983, **27**, 2111–2131.
101 G. van der Laan, *Phys. Rev. B: Condens. Matter Mater. Phys.*, 1990, **41**, 12366–12368.
102 F. M. F. de Groot, M. Grioni, J. C. Fuggle, J. Ghijsen, G. A. Sawatzky and H. Petersen, *Phys. Rev. B: Condens. Matter Mater. Phys.*, 1989, **40**, 5715–5723.
103 K. Watanabe, K. Inoue and F. Minami, *Phys. Rev. B: Condens. Matter Mater. Phys.*, 1992, **46**, 2024–2033.
104 L. Kavan, M. Grätzel, S. E. Gilbert, C. Klemenz and H. J. Scheel, *J. Am. Chem. Soc.*, 1996, **118**, 6716–6723.
105 J. Park, J. Joo, S. G. Kwon, Y. Jang and T. Hyeon, *Angew. Chem., Int. Ed.*, 2007, **46**, 4630–4660.
106 Y. Bessekhouad, D. Robert and J. V. Weber, *J. Photochem. Photobiol., A*, 2003, **157**, 47–53.
107 G. Oskam, A. Nellore, R. L. Penn and P. C. Searson, *J. Phys. Chem. B*, 2003, **107**, 1734–1738.
108 T. Sugimoto, *Adv. Colloid Interface Sci.*, 1987, **28**, 65–108.
109 M. A. Anderson, M. J. Gieselmann and Q. Xu, *J. Membr. Sci.*, 1988, **39**, 243–258.
110 E. A. Barringer and H. K. Bowen, *Langmuir*, 1985, **1**, 414–420.
111 J. H. Jean and T. A. Ring, *Langmuir*, 1986, **2**, 251–255.
112 C. Kormann, D. W. Bahnemann and M. R. Hoffmann, *J. Phys. Chem.*, 1988, **92**, 5196–5201.
113 J. Livage, M. Henry and C. Sanchez, *Prog. Solid State Chem.*, 1988, **18**, 259–341.
114 J.-L. Look and C. F. Zukoski, *J. Am. Ceram. Soc.*, 1995, **78**, 21–32.
115 J. L. Look and C. F. Zukoski, *J. Am. Ceram. Soc.*, 1992, **75**, 1587–1595.
116 B. O'Regan and M. Grätzel, *Nature*, 1991, **353**, 737–740.
117 R. L. Penn and J. F. Banfield, *Geochim. Cosmochim. Acta*, 1999, **63**, 1549–1557.
118 D. Vorkapic and T. Matsoukas, *J. Am. Ceram. Soc.*, 2005, **81**, 2815–2820.
119 D. Vorkapic and T. Matsoukas, *J. Colloid Interface Sci.*, 1999, **214**, 283–291.
120 C.-S. Kim, B. K. Moon, J.-H. Park, S. Tae Chung and S.-M. Son, *J. Cryst. Growth*, 2003, **254**, 405–410.
121 L. Miao, S. Tanemura, S. Toh, K. Kaneko and M. Tanemura, *J. Cryst. Growth*, 2004, **264**, 246–252.
122 M. S. Ghamsari, F. Hajiesmaeilbaigi and S. Mirdamadi, *Semicond. Phys., Quantum Electron. Optoelectron.*, 2007, **10**, 36–39.
123 Y. Lin, G. S. Wu, X. Y. Yuan, T. Xie and L. D. Zhang, *J. Phys.: Condens. Matter*, 2003, **15**, 2917–2922.
124 B. Liu and E. S. Aydil, *J. Am. Chem. Soc.*, 2009, **131**, 3985–3990.
125 T. Kasuga, M. Hiramatsu, A. Hoson, T. Sekino and K. Niihara, *Langmuir*, 1998, **14**, 3160–3163.
126 T. Kasuga, M. Hiramatsu, A. Hoson, T. Sekino and K. Niihara, *Adv. Mater.*, 1999, **11**, 1307–1311.
127 F. Sayilkan, *Turk. J. Chem.*, 2007, **31**, 211–221.
128 S. Y. Chae, M. K. Park, S. K. Lee, T. Y. Kim, S. K. Kim and W. I. Lee, *Chem. Mater.*, 2003, **15**, 3326–3331.

129 F. Cot, A. Larbot, G. Nabias and L. Cot, *J. Eur. Ceram. Soc.*, 1998, **18**, 2175–2181.
130 J. Yang, S. Mei and J. M. F. Ferreira, *J. Colloid Interface Sci.*, 2003, **260**, 82–88.
131 J. Yang, S. Mei and J. M. F. Ferreira, *Mater. Sci. Eng., C*, 2001, **15**, 183–185.
132 J. Yang, S. Mei and J. M. F. Ferreira, *J. Mater. Res.*, 2002, **17**, 2197–2200.
133 M. Rehan, X. Lai and G. M. Kale, *CrystEngComm*, 2011, **13**, 3725.
134 R. Vijayalakshmi and V. Rajendran, *Scholars Research Library*, 2012, **4**, 1183–1190.
135 Y. X. Zhang, G. H. Li, Y. X. Jin, Y. Zhang, J. Zhang and L. D. Zhang, *Chem. Phys. Lett.*, 2002, **365**, 300–304.
136 T. Kasuga, M. Hiramatsu, A. Hoson, T. Sekino and K. Niihara, *Adv. Mater.*, 1999, **11**, 1307–1311.
137 Z. Liu, Y. G. Andreev, A. Robert Armstrong, S. Brutti, Y. Ren and P. G. Bruce, *Prog. Nat. Sci.: Mater. Int.*, 2013, **23**, 235–244.
138 M. Cargnello, T. R. Gordon and C. B. Murray, *Chem. Rev.*, 2014, **114**, 9319–9345.
139 A. Craig and K. Gopal, *TiO_2 Nanotube Arrays, Synthesis, properties and Application*, Springer, Dordrecht Heidelberg, London, New York, 2009.
140 D. Gong, C. A. Grimes, O. K. Varghese, W. Hu, R. S. Singh, Z. Chen and E. C. Dickey, *J. Mater. Res.*, 2001, **16**, 3331–3334.
141 G. K. Mor, O. K. Varghese, M. Paulose and C. A. Grimes, *Sens. Lett.*, 2003, **1**, 42–46.
142 Q. Cai, M. Paulose, O. K. Varghese and C. A. Grimes, *J. Mater. Res.*, 2005, **20**, 230–236.
143 G. K. Mor, K. Shankar, O. K. Varghese and C. A. Grimes, *J. Mater. Res.*, 2004, **19**, 2989–2996.
144 V. Zwilling, M. Aucouturier and E. Darque-Ceretti, *Electrochim. Acta*, 1999, **45**, 921–929.
145 Y. Shimizu, N. Kuwano, T. Hyodo and M. Egashira, *Sens. Actuators, B*, 2002, **83**, 195–201.
146 J. Yamamoto, A. Tan, R. Shiratsuchi, S. Hayase, C. R. Chenthamarakshan and K. Rajeshwar, *Adv. Mater.*, 2003, **15**, 1823–1825.
147 G. Patermarakis, *J. Electrochem. Soc.*, 1995, **142**, 737.
148 K. Shankar, G. K. Mor, A. Fitzgerald and C. A. Grimes, *J. Phys. Chem. C*, 2007, **111**, 21–26.
149 C. Ruan, M. Paulose, O. K. Varghese and C. A. Grimes, *Sol. Energy Mater. Sol. Cells*, 2006, **90**, 1283–1295.
150 M. Paulose, K. Shankar, S. Yoriya, H. E. Prakasam, O. K. Varghese, G. K. Mor, T. A. Latempa, A. Fitzgerald and C. A. Grimes, *J. Phys. Chem. B*, 2006, **110**, 16179–16184.
151 S. Yoriya, G. K. Mor, S. Sharma and C. A. Grimes, *J. Mater. Chem.*, 2008, **18**, 3332.
152 R. Subasri, M. Tripathi, K. Murugan, J. Revathi, G. V. N. Rao and T. N. Rao, *Mater. Chem. Phys.*, 2010, **124**, 63–68.
153 Y. Yin, Z. Jin, F. Hou and X. Wang, *J. Am. Ceram. Soc.*, 2007, **90**, 2384–2389.
154 G. K. Mor, O. K. Varghese, M. Paulose, N. Mukherjee and C. A. Grimes, *J. Mater. Res.*, 2003, **18**, 2588–2593.
155 G. K. Mor, M. A. Carvalho, O. K. Varghese, M. V. Pishko and C. A. Grimes, *J. Mater. Res.*, 2004, **19**, 628–634.
156 G. K. Mor, K. Shankar, M. Paulose, O. K. Varghese and C. A. Grimes, *Nano Lett.*, 2005, **5**, 191–195.
157 O. K. Varghese, D. Gong, M. Paulose, C. A. Grimes and E. C. Dickey, *J. Mater. Res.*, 2003, **18**, 156–165.
158 S. Bauer, S. Kleber and P. Schmuki, *Electrochem. Commun.*, 2006, **8**, 1321–1325.
159 O. K. Varghese, D. Gong, M. Paulose, K. G. Ong, E. C. Dickey and C. A. Grimes, *Adv. Mater.*, 2003, **15**, 624–627.
160 L. K. Preethi, T. Mathews, M. Nand, S. N. Jha, C. S. Gopinath and S. Dash, *Appl. Catal., B*, 2017, **218**, 9–19.
161 S. Seifried, M. Winterer and H. Hahn, *Chem. Vap. Deposition*, 2000, **6**, 239–244.
162 J. A. Ayllón, A. Figueras, S. Garelik, L. Spirkova, J. Durand and L. Cot, *J. Mater. Sci. Lett.*, 1999, **18**, 1319–1321.
163 S. K. Pradhan, P. J. Reucroft, F. Yang and A. Dozier, *J. Cryst. Growth*, 2003, **256**, 83–88.
164 K. Okuyama, Y. Kousaka, N. Tohge, S. Yamamoto, J. J. Wu, R. C. Flagan and J. H. Seinfeld, *AIChE J.*, 1986, **32**, 2010–2019.
165 K. Okuyama, R. Ushio, Y. Kousaka, R. C. Flagan and J. H. Seinfeld, *AIChE J.*, 1990, **36**, 409–419.
166 K. Okuyama, J.-T. Jeung, Y. Kousaka, H. V. Nguyen, J. J. Wu and R. C. Flagan, *Chem. Eng. Sci.*, 1989, **44**, 1369–1375.
167 Z. Ding, X. Hu, G. Q. Lu, P.-L. Yue and P. F. Greenfield, *Langmuir*, 2000, **16**, 6216–6222.
168 J.-J. Wu and C.-C. Yu, *J. Phys. Chem. B*, 2004, **108**, 3377–3379.
169 D. G. Park and J. M. Burlitch, *Chem. Mater.*, 1992, **4**, 500–502.
170 H. D. Jang and S.-K. Kim, *Mater. Res. Bull.*, 2001, **36**, 627–637.
171 Y.-L. Li and T. Ishigaki, *Thin Solid Films*, 2002, **407**, 79–85.
172 S.-M. Oh and T. Ishigaki, *Thin Solid Films*, 2004, **457**, 186–191.
173 X. H. Wang, J.-G. Li, H. Kamiyama, M. Katada, N. Ohashi, Y. Moriyoshi and T. Ishigaki, *J. Am. Chem. Soc.*, 2005, **127**, 10982–10990.
174 M. Grujić-Brojčin, M. J. Šćepanović, Z. D. Dohčević-Mitrovi, I. Hinić, B. Matović, G. Stanišić and Z. V Popović, *J. Phys. D: Appl. Phys.*, 2005, **38**, 1415–1420.
175 M. Šćepanović, Z. Dohčević-Mitrović, I. Hinić, M. Grujić-Brojčin, G. Stanišić and Z. V. Popović, *Mater. Sci. Forum*, 2005, **494**, 265–270.
176 J.-M. Wu, H. C. Shih and W.-T. Wu, *Chem. Phys. Lett.*, 2005, **413**, 490–494.
177 J.-M. Wu, H. C. Shih, W.-T. Wu, Y.-K. Tseng and I.-C. Chen, *J. Cryst. Growth*, 2005, **281**, 384–390.
178 B. Xiang, Y. Zhang, Z. Wang, X. H. Luo, Y. W. Zhu, H. Z. Zhang and D. P. Yu, *J. Phys. D: Appl. Phys.*, 2005, **38**, 1152–1155.
179 H. Zhang, X. Luo, J. Xu, B. Xiang and D. Yu, *J. Phys. Chem. B*, 2004, **108**, 14866–14869.
180 J.-M. Wu, H. C. Shih and W.-T. Wu, *Nanotechnology*, 2006, **17**, 105–109.

181 D. K. Hwang, J. H. Moon, Y. G. Shul, K. T. Jung, D. H. Kim and D. W. Lee, *J. Sol-Gel Sci. Technol.*, 2003, **26**, 783–787.
182 J.-W. Kim, J.-W. Shim, J.-H. Bae, S.-H. Han, H.-K. Kim, I.-S. Chang, H.-H. Kang and K.-D. Suh, *Colloid Polym. Sci.*, 2002, **280**, 584–588.
183 B. Mahltig, H. Böttcher, K. Rauch, U. Dieckmann, R. Nitsche and T. Fritz, *Thin Solid Films*, 2005, **485**, 108–114.
184 A. P. Popov, A. V Priezzhev, J. Lademann and R. Myllylä, *J. Phys. D: Appl. Phys.*, 2005, **38**, 2564–2570.
185 C. E. Sittig, Charakterisierung der Oxidschichten auf Titan und Titanlegierungen sowie deren Reaktionen in Kontact mit biologisch relevanten Modellösungen, PhD thesis, ETH Nr, 12657, Zürich, 1998.
186 W. Clark and P. Broadhead, *J. Phys. C: Solid State Phys.*, 1970, **3**, 1047.
187 R. Wang, K. Hashimoto, A. Fujishima, M. Chikuni, E. Kojima, A. Kitamura, M. Shimohigoshi and T. Watanabe, *Nature*, 1997, **388**, 431–432.
188 A. Fujishima, X. Zhang and D. Tryk, *Surf. Sci. Rep.*, 2008, **63**, 515–582.
189 Y. Xie, *Electrochim. Acta*, 2006, **51**, 3399–3406.
190 Y. Lai, L. Sun, Y. Chen, H. Zhuang, C. Lin and J. W. Chin, *J. Electrochem. Soc.*, 2006, **153**, D123.
191 N. M. Mahmoodi, M. Arami, N. Y. Limaee and N. S. Tabrizi, *Chem. Eng. J.*, 2005, **112**, 191–196.
192 A.-P. Zhang, *World J. Gastroenterol.*, 2004, **10**, 3191–3193.
193 A. O. Ibhadon, Multifunctional TiO_2 Catalysis and Applications, in *Proceedings of Green Chemistry and Engineering International Conference*, Washington, DC, USA, 24–26 June 2008.
194 C.-C. Wang, Z. Zhang and J. Y. Ying, *Nanostruct. Mater.*, 1997, **9**, 583–586.
195 J.-M. Wu, T.-W. Zhang, Y.-W. Zeng, S. Hayakawa, K. Tsuru and A. Osaka, *Langmuir*, 2005, **21**, 6995–7002.
196 T. Peng, D. Zhao, K. Dai, W. Shi and K. Hirao, *J. Phys. Chem. B*, 2005, **109**, 4947–4952.
197 S. Yang, X. Quan, X. Li, N. Fang, N. Zhang and H. Zhao, *J. Environ. Sci.*, 2005, **17**, 290–293.
198 Y. Bessekhouad, D. Robert, J.-V. Weber and N. Chaoui, *J. Photochem. Photobiol., A*, 2004, **167**, 49–57.
199 Y. Cao, W. Yang, W. Zhang, G. Liu and P. Yue, *New J. Chem.*, 2004, **28**, 218.
200 W. Li, Y. Wang, H. Lin, S. Ismat Shah, C. P. Huang, D. J. Doren, S. A. Rykov, J. G. Chen and M. A. Barteau, *Appl. Phys. Lett.*, 2003, **83**, 4143–4145.
201 S. Peng, Y. Li, F. Jiang, G. Lu and S. Li, *Chem. Phys. Lett.*, 2004, **398**, 235–239.
202 Y. Sakatani, H. Ando, K. Okusako, H. Koike, J. Nunoshige, T. Takata, J. N. Kondo, M. Hara and K. Domen, *J. Mater. Res.*, 2004, **19**, 2100–2108.
203 X. Zhang and L. Lei, *Mater. Lett.*, 2008, **62**, 895–897.
204 M. S. Nahar, K. Hasegawa and S. Kagaya, *Chemosphere*, 2006, **65**, 1976–1982.
205 K. Iketani, R.-D. Sun, M. Toki, K. Hirota and O. Yamaguchi, *Mater. Sci. Eng., B*, 2004, **108**, 187–193.
206 J. Zhu, F. Chen, J. Zhang, H. Chen and M. Anpo, *J. Photochem. Photobiol., A*, 2006, **180**, 196–204.
207 D. Hyun Kim, K. Sub Lee, Y.-S. Kim, Y.-C. Chung and S.-J. Kim, *J. Am. Ceram. Soc.*, 2006, **89**, 515–518.
208 J. C.-S. Wu and C.-H. Chen, *J. Photochem. Photobiol., A*, 2004, **163**, 509–515.
209 C.-C. Pan and J. C. S. Wu, *Mater. Chem. Phys.*, 2006, **100**, 102–107.
210 S. Kim, S.-J. Hwang and W. Choi, *J. Phys. Chem. B*, 2005, **109**, 24260–24267.
211 R. Amadelli, L. Samiolo, A. Maldotti, A. Molinari, M. Valigi and D. Gazzoli, *Int. J. Photoenergy*, 2008, **2008**, 1–9.
212 T. Lindgren, J. M. Mwabora, E. Avendaño, J. Jonsson, A. Hoel, C.-G. Granqvist and S.-E. Lindquist, *J. Phys. Chem. B*, 2003, **107**, 5709–5716.
213 C. Burda, Y. Lou, X. Chen, A. C. S. Samia, J. Stout and J. L. Gole, *Nano Lett.*, 2003, **3**, 1049–1051.
214 X. Chen, Y.-B. Lou, A. C. S. Samia, C. Burda and J. L. Gole, *Adv. Funct. Mater.*, 2005, **15**, 41–49.
215 Y. Choi, T. Umebayashi and M. Yoshikawa, *J. Mater. Sci.*, 2004, **39**, 1837–1839.
216 H. Irie, Y. Watanabe and K. Hashimoto, *Chem. Lett.*, 2003, **32**, 772–773.
217 Y. Xie, L. M. Zhou and H. Huang, *Mater. Lett.*, 2006, **60**, 3558–3560.
218 S. Sakthivel, M. Janczarek and H. Kisch, *J. Phys. Chem. B*, 2004, **108**, 19384–19387.
219 H. Tokudome and M. Miyauchi, *Chem. Lett.*, 2004, **33**, 1108–1109.
220 C. Shifu, C. Lei, G. Shen and C. Gengyu, *Chem. Phys. Lett.*, 2005, **413**, 404–409.
221 O. Diwald, T. L. Thompson, T. Zubkov, S. D. Walck and J. T. Yates, *J. Phys. Chem. B*, 2004, **108**, 6004–6008.
222 T. Ohno, M. Akiyoshi, T. Umebayashi, K. Asai, T. Mitsui and M. Matsumura, *Appl. Catal., A*, 2004, **265**, 115–121.
223 M. Shen, Z. Wu, H. Huang, Y. Du, Z. Zou and P. Yang, *Mater. Lett.*, 2006, **60**, 693–697.
224 J. C. Yu, J. Yu, W. Ho, Z. Jiang and L. Zhang, *Chem. Mater.*, 2002, **14**, 3808–3816.
225 D. Li, H. Haneda, N. K. Labhsetwar, S. Hishita and N. Ohashi, *Chem. Phys. Lett.*, 2005, **401**, 579–584.
226 D. Li, H. Haneda, S. Hishita, N. Ohashi and N. K. Labhsetwar, *J. Fluorine Chem.*, 2005, **126**, 69–77.
227 M. Grätzel, *Nature*, 2001, **414**, 338–344.
228 F. Cao, G. Oskam, G. J. Meyer and P. C. Searson, *J. Phys. Chem.*, 1996, **100**, 17021–17027.
229 A. Solbrand, H. Lindström, H. Rensmo, A. Hagfeldt, S.-E. Lindquist and S. Södergren, *J. Phys. Chem. B*, 1997, **101**, 2514–2518.
230 M. Ni, M. K. H. Leung, D. Y. C. Leung and K. Sumathy, *Renewable Sustainable Energy Rev.*, 2007, **11**, 401–425.
231 A. Kudo and Y. Miseki, *Chem. Soc. Rev.*, 2009, **38**, 253–278.
232 A. Hameed and M. A. Gondal, *J. Mol. Catal. A: Chem.*, 2004, **219**, 109–119.
233 A. Yamakata, T. Ishibashi and H. Onishi, *J. Mol. Catal. A: Chem.*, 2003, **199**, 85–94.
234 W. Y. Teoh, J. A. Scott and R. Amal, *J. Phys. Chem. Lett.*, 2012, **3**, 629–639.

235 M. S. Wrighton, A. B. Ellis, P. T. Wolczanski, D. L. Morse, H. B. Abrahamson and D. S. Ginley, *J. Am. Chem. Soc.*, 1976, **98**, 2774–2779.
236 Z.-L. Jin and G.-X. Lu, *Energy Fuels*, 2005, **19**, 1126–1132.
237 S. U. M. Khan, M. Al-Shahry and W. B. Ingler, *Science*, 2002, **297**, 2243–2245.
238 M. Matsuoka, M. Kitano, M. Takeuchi, M. Anpo and J. M. Thomas, *Top. Catal.*, 2005, **35**, 305–310.
239 M. Matsuoka, M. Kitano, M. Takeuchi, M. Anpo and J. M. Thomas, *Mater. Sci. Forum*, 2005, **486–487**, 81–84.
240 D. Bocharov, S. Piskunov, Y. F. Zhukovskii, E. Spohr and P. N. D'yachkov, *Vacuum*, 2017, **146**, 562–569.
241 J. F. Guayaquil-Sosa, B. Serrano-Rosales, P. J. Valadés-Pelayo and H. de Lasa, *Appl. Catal., B*, 2017, **211**, 337–348.
242 M. Alitabar and H. Yoozbashizadeh, *Mater. Res. Bull.*, 2017, **95**, 169–176.
243 K. Dhanalakshmi, *Int. J. Hydrogen Energy*, 2001, **26**, 669–674.
244 R. Argazzi, N. Y. Murakami Iha, H. Zabri, F. Odobel and C. A. Bignozzi, *Coord. Chem. Rev.*, 2004, **248**, 1299–1316.
245 A. S. Polo, M. K. Itokazu and N. Y. Murakami Iha, *Coord. Chem. Rev.*, 2004, **248**, 1343–1361.
246 D. Duonghong, E. Borgarello and M. Graetzel, *J. Am. Chem. Soc.*, 1981, **103**, 4685–4690.
247 T. Sreethawong, C. Junbua and S. Chavadej, *J. Power Sources*, 2009, **190**, 513–524.
248 Y. Li, C. Xie, S. Peng, G. Lu and S. Li, *J. Mol. Catal. A: Chem.*, 2008, **282**, 117–123.
249 K. K. Mandari, B. S. Kwak, A. K. R. Police and M. Kang, *Mater. Res. Bull.*, 2017, **95**, 515–524.
250 H. Zhang, F. Liu, H. Wu, X. Cao, J. Sun and W. Lei, *RSC Adv.*, 2017, **7**, 40327–40333.
251 B. Hou, L. Shen, H. Shi, R. Kapadia and S. B. Cronin, *Phys. Chem. Chem. Phys.*, 2017, **19**, 2877–2881.
252 J. Zhang, Z. Yu, Z. Gao, H. Ge, S. Zhao, C. Chen, S. Chen, X. Tong, M. Wang, Z. Zheng and Y. Qin, *Angew. Chem., Int. Ed.*, 2017, **56**, 816–820.
253 H. Xu, S. Li, L. Ge, C. Han, Y. Gao and D. Dai, *Int. J. Hydrogen Energy*, 2017, **42**, 22877–22886.
254 Y. Sui, S. Liu, T. Li, Q. Liu, T. Jiang, Y. Guo and J.-L. Luo, *J. Catal.*, 2017, **353**, 250–255.
255 J. Si, Y. Wang, X. Xia, S. Peng, Y. Wang, S. Xiao, L. Zhu, Y. Bao, Z. Huang and Y. Gao, *J. Power Sources*, 2017, **360**, 353–359.
256 M. Wang, Z. Li, Y. Wu, J. Ma and G. Lu, *J. Catal.*, 2017, **353**, 162–170.
257 R. Liu, Z. Sun, X. Song, Y. Zhang, L. Xu and L. Xi, *Appl. Catal., A*, 2017, **544**, 137–144.
258 P. V Kamat and D. Meisel, *Curr. Opin. Colloid Interface Sci.*, 2002, **7**, 282–287.
259 W. Choi, J. Lee, S. Kim, S. Hwang, M. C. Lee and T. K. Lee, *J. Ind. Eng. Chem.*, 2003, **9**, 96–101.
260 H. Hussain, G. Tocci, T. Woolcot, X. Torrelles, C. L. Pang, D. S. Humphrey, C. M. Yim, D. C. Grinter, G. Cabailh, O. Bikondoa, R. Lindsay, J. Zegenhagen, A. Michaelides and G. Thornton, *Nat. Mater.*, 2017, **16**(4), 461–466.
261 P. Salvador, *New J. Chem.*, 1988, **12**, 35–43.
262 E. Liu, L. Kang, Y. Yang, T. Sun, X. Hu, C. Zhu, H. Liu, Q. Wang, X. Li and J. Fan, *Nanotechnology*, 2014, **25**, 165401.
263 K. Nishijima, T. Kamai, N. Murakami, T. Tsubota and T. Ohno, *Int. J. Photoenergy*, 2008, **2008**, 1–7.
264 Y.-S. Chen and P. V. Kamat, *J. Am. Chem. Soc.*, 2014, **136**, 6075–6082.
265 Z. Yang, D. Choi, S. Kerisit, K. M. Rosso, D. Wang, J. Zhang, G. Graff and J. Liu, *J. Power Sources*, 2009, **192**, 588–598.
266 P. G. Bruce, B. Scrosati and J.-M. Tarascon, *Angew. Chem., Int. Ed.*, 2008, **47**, 2930–2946.
267 A. S. Aricò, P. Bruce, B. Scrosati, J.-M. Tarascon and W. van Schalkwijk, *Nat. Mater.*, 2005, **4**, 366–377.
268 D. Panduwinata and J. D. Gale, *J. Mater. Chem.*, 2009, **19**, 3931–3940.
269 C. Arrouvel, S. C. Parker and M. S. Islam, *Chem. Mater.*, 2009, **21**, 4778–4783.
270 C.-C. Tsai and H. Teng, *Chem. Mater.*, 2006, **18**, 367–373.
271 H. Miyazaki, T. Hyodo, Y. Shimizu and M. Egashira, *Sens. Actuators, B*, 2005, **108**, 467–472.
272 A. M. Ruiz, A. Cornet and J. R. Morante, *Sens. Actuators, B*, 2004, **100**, 256–260.
273 S. El-Sherbiny, F. Morsy, M. Samir and O. A. Fouad, *Appl. Nanosci.*, 2014, **4**, 305–313.
274 R. I Bickley, T. Gonzalezcarreno, J. S. Lees, L. Palmisano and R. J. D. Tilley, *J. Solid State Chem.*, 1991, **92**, 178–190.
275 R. Comparelli, E. Fanizza, M. L. Curri, P. D. Cozzoli, G. Mascolo, R. Passino and A. Agostiano, *Appl. Catal., B*, 2005, **55**, 81–91.
276 X. Chen and S. S. Mao, *Chem. Rev.*, 2007, **107**, 2891–2959.
277 M. Pelaez, N. T. Nolan, S. C. Pillai, M. K. Seery, P. Falaras, A. G. Kontos, P. S. M. Dunlop, J. W. J. Hamilton, J. A. Byrne, K. O'Shea, *et al.*, *Appl. Catal., B*, 2012, **125**, 331–349.
278 M. Long, L. Zheng, B. Tan and H. Shu, *Appl. Surf. Sci.*, 2016, **386**, 434–441.
279 Y. Ben-Shahar and U. Banin, *Top. Curr. Chem.*, 2016, **374**, 54.
280 S. Murgolo, F. Petronella, R. Ciannarella, R. Comparelli, A. Agostiano, M. L. Curri and G. Mascolo, *Catal. Today*, 2015, **240**, 114–124.
281 Y. Tang, G. Zhang, C. Liu, S. Luo, X. Xu, L. Chen and B. Wang, *J. Hazard. Mater.*, 2013, **252–253**, 115–122.
282 F. Petronella, A. Truppi, C. Ingrosso, T. Placido, M. Striccoli, M. L. Curri, A. Agostiano and R. Comparelli, *Catal. Today*, 2017, **281**, 85–100.
283 L. Karimi, M. E. Yazdanshenas, R. Khajavi, A. Rashidi and M. Mirjalili, *Cellulose*, 2014, **21**, 3813–3827.
284 F. Petronella, A. Truppi, T. Sibillano, C. Giannini, M. Striccoli, R. Comparelli and M. L. Curri, *Catalysts*, 2017, **7**, 100.
285 L. Carbone and P. D. Cozzoli, *Nano Today*, 2010, **5**, 449–493.
286 Á. Kmetykó, Á. Szániel, C. Tsakiroglou, A. Dombi and K. Hernádi, *React. Kinet., Mech. Catal.*, 2016, **117**, 379–390.
287 R. Su, R. Tiruvalam, Q. He, N. Dimitratos, L. Kesavan, C. Hammond, J. A. Lopez-Sanchez, R. Bechstein, C. J. Kiely, G. J. Hutchings, *et al.*, *ACS Nano*, 2012, **6**, 6284–6292.

288 A. Takai and P. V. Kamat, *ACS Nano*, 2011, **5**, 7369–7376.
289 L. Francioso, D. S. Presicce, P. Siciliano and A. Ficarella, *Sens. Actuators, B*, 2007, **123**, 516–521.
290 Y. Mizukoshi, Y. Makise, T. Shuto, J. Hu, A. Tominaga, S. Shironita and S. Tanabe, *Ultrason. Sonochem.*, 2007, **14**, 387–392.
291 H. Wang, T. You, W. Shi, J. Li and L. Guo, *J. Phys. Chem. C*, 2012, **116**, 6490–6494.
292 R. S. Sonawane and M. K. Dongare, *J. Mol. Catal. A: Chem.*, 2006, **243**, 68–76.
293 G. L. Chiarello, E. Selli and L. Forni, *Appl. Catal., B*, 2008, **84**, 332–339.
294 F. Wenqing, L. Qinghua, Z. Qinghong and W. Ye, *J. Phys. Chem. C*, 2011, **115**, 10694–10701.
295 J. Deepa, M. S. Christopher, S. R. Sadhana, M. S. Khadga and J. K. Kenneth, *Int. J. Photoenergy*, 2013, **2013**, 10.
296 G. Anna and W. Jerzy, *Energy Fuels*, 2005, **3**, 1143–1147.
297 V. I. Yatskiv, A. V. Korzhak, V. M. Granchak, A. S. Kovalenko and S. Ya. Kuchmiy, *Theor. Exp. Chem.*, 2003, **39**, 167–171.
298 Š. Václav and K. Daniela, *Int. J. Photoenergy*, 2011, **2011**, 14.
299 X. Quanjun, Y. Jiaguo and J. Mietek, *J. Am. Chem. Soc.*, 2012, **15**, 6575–6578.
300 V. K. Anna, I. E. Natalia, L. S. Alexander, K. B. Viktor, E. R. Alexandra, I. L. Valentina, Y. Stepan, V. G. I. Kuchmiy and A. M. Piotr, *J. Photochem. Photobiol., A*, 2008, **198**, 126–134.
301 D. Ke, P. Tianyou, Ke. Dingning and W. Bingqing, *Nanotechnology*, 2009, **20**, 12.
302 M. Takuya, K. Satoshi, K. Hideyuki, S. Tohru, O. Kiyohisa, C. V. Suresh and S. Kunihiro, *Int. J. Hydrogen Energy*, 2010, **35**, 6554–6560.
303 R. Nitish, T. L. Kam and P. Debabrata, *J. Phys. Chem. C*, 2015, **33**, 19117–19125.
304 Z. Lu, T. Baozhu, C. Feng and Z. Jinlong, *Int. J. Hydrogen Energy*, 2012, **37**, 17060–17067.
305 P. Fuyun, L. Yingliang, X. Shengang, L. Jing, W. Chenxu and C. Shaokui, *Int. J. Hydrogen Energy*, 2013, **38**, 2670–2677.
306 K. Yang, C. Meng, L. Lin, X. Peng, X. Chen, X. Wang, W. Dai and X. Fu, *Catal. Sci. Technol.*, 2016, **6**, 829–839.
307 E. Kowalska, Z. Wei, B. Karabiyik, A. Herissan, M. Janczarek, M. Endo, A. Markowska-Szczupak, H. Remita and B. Ohtani, *Catal. Today*, 2015, **252**, 136–142.
308 S. W. Verbruggen, M. Keulemans, M. Filippousi, D. Flahaut, G. van Tendeloo, S. Lacombe, J. A. Martens and S. Lenaerts, *Appl. Catal., B*, 2014, **156–157**, 116–121.
309 X. Qiu, M. Miyauchi, K. Sunada, M. Minoshima, M. Liu, Y. Lu, D. Li, Y. Shimodaira, Y. Hosogi and Y. Kuroda, *ACS Nano*, 2012, **6**, 1609–1618.
310 Y. Wang, F. Pan, W. Dong, L. Xu, K. Wu, G. Xu and W. Chen, *Appl. Catal., B*, 2016, **189**, 192–198.
311 S. Mallakpour and E. Khadem, *Chem. Eng. J.*, 2016, **302**, 344–367.
312 M. Horn, C. F. Schwerdtfeger and E. P. Meagher, *Z. Kristallogr.*, 1972, **136**, 273–281.
313 H. Tang, *Electronic Properties of Anatase TiO_2 Investigated by Electrical and Optical Measurements on Single Crystals and Thin Films*, Département de physique, Ecole polytechnique fédérale de Lausanne EPFL, Lausanne, France, 1994.
314 N. Tsuda, K. Nasu, A. Yanase and K. Siratori, *Electronic Conduction in Oxides*, Springer-Verlag, Berlin, Gerseveral, 1991.
315 A. Eucken and W. Dannöhl, Die thermisce Ausdehnung einiger Alkalihalogenide and Metalle bei hohen Temperaturen, *Z. Elektrochem.*, 1934, **40**, 814–821.
316 M. S. Lee, S.-S. Hong and M. Mohseni, *J. Mol. Catal. A: Chem.*, 2005, **242**, 135–140.
317 J. O. Carneiro, V. Teixeira, A. Portinha, L. Dupák, A. Magalhães and P. Coutinho, *Vacuum*, 2005, **78**, 37–46.
318 J. C.-S. Wu and C.-H. Chen, *J. Photochem. Photobiol., A*, 2004, **163**, 509–515.
319 X. Z. Li and F. B. Li, *Environ. Sci. Technol.*, 2001, **35**, 2381–2387.
320 F. B. Li and X. Z. Li, *Chemosphere*, 2002, **48**, 1103–1111.
321 Z. Wu, F. Dong, W. Zhao and S. Guo, *J. Hazard. Mater.*, 2008, **157**, 57–63.
322 R. Asahi, *Science*, 2001, **293**, 269–271.
323 K. Takeshita, A. Yamakata, T. Ishibashi, H. Onishi, K. Nishijima and T. Ohno, *J. Photochem. Photobiol., A*, 2006, **177**, 269–275.
324 J. Yu, M. Zhou, B. Cheng and X. Zhao, *J. Mol. Catal. A: Chem.*, 2006, **246**, 176–184.
325 S. Y. Treschev, P.-W. Chou, Y.-H. Tseng, J.-B. Wang, E. V. Perevedentseva and C.-L. Cheng, *Appl. Catal., B*, 2008, **79**, 8–16.
326 C. Lettmann, K. Hildenbrand, H. Kisch, W. Macyk and W. F. Maier, *Appl. Catal., B*, 2001, **32**, 215–227.
327 A. Zaleska, J. W. Sobczak, E. Grabowska and J. Hupka, *Appl. Catal., B*, 2008, **78**, 92–100.
328 L. Kőrösi and I. Dékány, *Colloids Surf., A*, 2006, **280**, 146–154.
329 K. Sayama and H. Arakawa, *J. Chem. Soc., Faraday Trans.*, 1997, **93**, 1647–1654.
330 K. Sayama and H. Arakawa, *J. Phys. Chem.*, 1993, **97**, 531–533.
331 A. Kudo, H. Kato and S. Nakagawa, *J. Phys. Chem. B*, 2000, **104**, 571–575.
332 H. Kato and A. Kudo, *Chem. Phys. Lett.*, 1998, **295**, 487–492.
333 K. Sayama, H. Arakawa and K. Domen, *Catal. Today*, 1996, **28**, 175–182.
334 K. Fujihara, T. Ohno and M. Matsumura, *J. Chem. Soc., Faraday Trans.*, 1998, **94**, 3705–3709.
335 R. Abe, T. Takata, H. Sugihara and K. Domen, *Chem. Commun.*, 2005, 3829–3931.
336 M. Higashi, R. Abe, T. Takata and K. D omen, *Chem. Mater.*, 2009, **21**, 1543–1549.
337 H. Kato, M. Hori, R. Konta, Y. Shimodaira and A. Kudo, *Chem. Lett.*, 2004, **33**, 1348–1349.
338 L. B. Fen, T. K. Han, M. Nee, B. C. Ang and M. R. Johan, *Appl. Surf. Sci.*, 2011, **258**, 431–435.